

1

2 **Drift barriers to quality control when genes are expressed at different levels**

3 Xiong K<sup>\*</sup>, McEntee JP<sup>†</sup>, Porfirio DJ<sup>‡</sup>, Masel J<sup>†</sup>

4

5 <sup>\*</sup>Department of Molecular & Cellular Biology, <sup>†</sup>Department of Ecology & Evolutionary

6 Biology, <sup>‡</sup>Department of Computer Science, University of Arizona, Tucson AZ 85721

- 7 Corresponding author: Joanna Masel 1041 E Lowell St, Tucson AZ 85721 USA
- 8 masel@email.arizona.edu Ph. +1 520-626-9888
- 9 Running title: Drift barriers to quality control
- 10 Keywords: cryptic genetic variation, stop codon readthrough, robustness, evolvability,
- 11 transcriptional errors, proofreading

12

## ABSTRACT

13 Gene expression is imperfect, sometimes leading to toxic products. Solutions take two forms:  
14 globally reducing error rates, or ensuring that the consequences of erroneous expression are  
15 relatively harmless. The latter is optimal, but because it must evolve independently at so many  
16 loci, it is subject to a stringent “drift barrier” – a limit to how weak the effects of a deleterious  
17 mutation  $s$  can be, while still being effectively purged by selection, expressed in terms of the  
18 population size  $N$  of an idealized population such that purging requires  $s < -1/N$ . In previous  
19 work, only large populations evolved the optimal local solution, small populations instead  
20 evolved globally low error rates, and intermediate populations were bistable, with either  
21 solution possible. Here we take into consideration the fact that the effectiveness of purging  
22 varies among loci, because of variation in gene expression level and variation in the intrinsic  
23 vulnerabilities of different gene products to error. The previously found dichotomy between  
24 the two kinds of solution breaks down, replaced by a gradual transition as a function of  
25 population size. In the extreme case of a small enough population, selection fails to maintain  
26 even the global solution against deleterious mutations, explaining the non-monotonic  
27 relationship between effective population size and transcriptional error rate that was recently  
28 observed in experiments on *E. coli*, *C. elegans* and *Buchnera aphidicola*.

29  
30  
31  
32  
33  
34  
35  
36  
37  
38  
39  
40  
41  
42  
43  
44  
45  
46  
47  
48  
49  
50

## INTRODUCTION

In classical population genetic models of idealized populations, the probability of fixation of a new mutant depends sharply on the product of the selection coefficient  $s$  and the population size  $N$ . As  $s$  falls below  $-1/N$ , fixation probabilities drop exponentially, corresponding to efficient selective purging of deleterious mutations. For  $s > -1/N$ , random genetic drift makes the fate of new mutants less certain. This nonlinear dependence of fixation probability on  $sN$  has given rise to the “drift barrier” hypothesis (Lynch 2007), which holds that populations are characterized by a threshold or “barrier” value of the selection coefficient  $s$ , corresponding to the tipping point at which the removal of deleterious mutations switches between effective and ineffective. In idealized populations described by Wright-Fisher or Moran models, the drift barrier is positioned at  $s = \sim -1/N$ . Drift barriers also exist, albeit sometimes with less abrupt threshold behavior, in more complex models of evolution in which some assumptions of an idealized population are relaxed (Good and Desai 2014).

The drift barrier theory argues that variation among species in their characteristic threshold values for  $s$ , thresholds that are equal by definition to the inverse of the selection effective population size  $N_e$ , can explain why different species have different characteristics, e.g. streamlined versus bloated genomes (Lynch 2007). The simplest interpretation of the drift barrier would seem to imply that large- $N_e$  species show stricter quality control over all biological processes, e.g. higher fidelity in DNA replication, transcription, and translation, than small- $N_e$  species, because molecular defects in quality control mechanisms are less effectively purged in the latter (Lynch 2010; Traverse and Ochman 2016a).

51 However, the data reveals more complex patterns. Unsurprisingly, *Buchnera aphidicola*, which  
52 has exceptionally low  $N_e$  (Mira and Moran 2002; Rispe *et al.* 2004), has a higher transcriptional  
53 error rate, at  $4.67 \times 10^{-5}$  (Traverse and Ochman 2016b), than the error rate  $4.1 \times 10^{-6}$  previously  
54 reported for *Caenorhabditis elegans* (Gout *et al.* 2013). But to the surprise of the authors, the  
55 error rate in large- $N_e$  *Escherichia coli* is highest of all, at  $8.23 \times 10^{-5}$  (Traverse and Ochman  
56 2016b).

57

58 A more refined drift barrier theory can explain these findings. As the fitness burden  
59 accumulates from the slightly deleterious mutations that a small- $N_e$  species cannot purge,  
60 some forms of quality control may evolve as a second line of defense. The ideal solution is to  
61 purge all deleterious mutations, even those of tiny effect; when this first line of defense fails,  
62 the second line of defense is to ameliorate the cumulative phenotypic consequences of the  
63 deleterious mutations that have accumulated (Frank 2007; Rajon and Masel 2011; Warnecke  
64 and Hurst 2011; Lynch 2012; Wu and Hurst 2015). In some circumstances, as described further  
65 below, strict quality control can act as such an amelioration strategy (Rajon and Masel 2011).  
66 The existence of two distinct lines of defense complicates the naive drift barrier logic that large-  
67  $N_e$  species should generally exhibit stricter quality control in all molecular processes. The  
68 superior performance of large- $N_e$  species in a primary line of defense other than quality control  
69 may remove any advantage of strict and costly quality control as a secondary line of defense.  
70 This creates a seemingly counter-intuitive pattern in quality control, in which small- $N_e$  species  
71 can evolve more faithful processes than large- $N_e$  species such as *E. coli*.

72

73 The existence of two substantively different lines of defense was first proposed by Krakauer  
74 and Plotkin (2002), who contrasted the “redundancy” of robustness to the consequences of  
75 mutational errors with the “antiredundancy” of hypersensitivity to mutations. By positing that  
76 redundancy had a cost, they showed that the superior cost-free solution of antiredundancy was  
77 available only with large  $N_e$ , giving small- $N_e$  species higher levels of “redundancy”.

78  
79 A related argument was made by Rajon and Masel (2011) in the context of mitigating the harms  
80 threatened by errors in molecular processes such as translation. Rajon and Masel (2011)  
81 distinguished between “local” solutions, where a separate solution is required at each locus,  
82 and “global” solutions that can deal with problems at many loci simultaneously. The evolution  
83 of extensive quality control mechanisms was deemed a global solution because a single  
84 mutation impacting general quality control mechanisms can affect the prevention of gene  
85 expression errors at many loci. Note that quality control includes not only mechanisms such as  
86 proofreading for preventing errors from happening in the first place, but also mechanisms that  
87 reduce downstream damage from errors, e.g. degradation of mRNA molecules that seem faulty.  
88 Global quality control should come with a cost in time or energy. The alternative, local solution  
89 is to have a benign rather than a strongly deleterious “cryptic genetic sequence” at each locus  
90 at which expression errors might occur, making the consequence of an error at that locus  
91 relatively harmless. In contrast to the global solution, these local solutions bear no direct fitness  
92 cost, but because selection at any one locus is weak, mutations at any one locus pass more  
93 easily through the drift barrier, making them more difficult to maintain than global solutions.

94

95 Both the quality control of Rajon and Masel (2011) and the “redundancy” of Krakauer and  
96 Plotkin (2002) to the consequences of mutations are global across loci, and also costly (the  
97 former costly by design, the latter costly as a consequence of scaling decisions). Meantime,  
98 both the “local” solutions of Rajon and Masel (2011) and the “antiredundancy” of Krakauer and  
99 Plotkin (2002) carry no true fitness cost but instead require a large- $N_e$  drift barrier and/or face a  
100 “cost of selection” (Haldane 1957) as limits to their adaptation. A mutation disrupting a solution  
101 specific to a single locus requires a large value of  $N_e$  for its purging, whereas a mutation  
102 disrupting a global quality control mechanism will have large fitness consequences and so be  
103 easier to purge. The higher-fitness solution is the local one, but it is evolutionarily achievable  
104 only with large  $N_e$ . With small  $N_e$ , we instead expect global solutions such as extensive (and  
105 costly) quality control.

106  
107 Selection to achieve the local solution by purging deleterious mutations to cryptic sequences  
108 (leaving in place genotypes whose cryptic genetic sequences are benign) may be difficult and  
109 hence restricted to high- $N_e$  populations. There are, however, reasons to believe that it is not  
110 impossible. For example, when the error in question is reading through a stop codon, the local  
111 cryptic genetic sequence is the 3'UTR, which is read by the ribosome. One option for a more  
112 benign form of this cryptic sequence is the presence of a “backup” stop codon that provides the  
113 ribosome with a second and relatively early chance to terminate translation. Such backup stops  
114 are common at the first position past the stop in prokaryotes (Nichols 1970). In *Saccharomyces*  
115 *cerevisiae*, there is also an abundance of stop codons at the third codon position past the stop  
116 (Williams *et al.* 2004). Moreover, conservation at this position depends strongly on whether or

117 not the codon is a stop, and the overrepresentation of stops at this position is greater in more  
118 highly expressed genes (Liang *et al.* 2005). In some ciliates, where the genetic code has been  
119 reassigned so that UAA and UAG correspond to glutamine, this overrepresentation is much  
120 more pronounced (Adachi and Cavalcanti 2009). As with the consequences of erroneous  
121 readthrough, selective pressure on erroneous amino acid misincorporation and/or misfolding  
122 (Drummond and Wilke 2008), and on erroneous protein-protein interactions (Brettner and  
123 Masel 2012) are also strong enough to shape protein expression and interaction patterns. In  
124 the case of transcriptional errors, while both *E. coli* and *B. aphidicola* have high error rates, only  
125 *E. coli* shows signs of having evolved a first line of defense in the form of a decreased frequency  
126 with which observed transcriptional errors translate into non-synonymous changes, relative to  
127 randomly sampled transcriptional errors (Traverse and Ochman 2016a).

128  
129 Rajon and Masel (2011) found that for intermediate values of  $N_e$  that correspond strikingly well  
130 to many multicellular species of interest, the evolutionary dynamics of the system were  
131 bistable, with either the global or the local solution possible. This is a natural consequence of a  
132 positive feedback loop; in the presence of a strict global quality control mechanism, specialized  
133 solutions at particular loci are unnecessary and mutations destroying them pass through the  
134 drift barrier (we use the expression “pass through the drift barrier” to mean that  $0 > s > -1/N$ ),  
135 with their subsequent absence increasing the demand for quality control. Similarly, when  
136 specialized solutions predominate, the advantage to quality control is lessened, and resulting  
137 higher error rates further increase selection for many locally specialized solutions. If true, this



138 bistability suggests that historical contingency, rather than current values of  $N_e$ , determine  
139 which processes are error-prone vs. high-fidelity for populations at intermediate  $N_e$ .

140  
141 In the current work, we note that the model of Rajon and Masel (2011) contained an unrealistic  
142 symmetry, namely that the fitness consequence of a molecular error at one locus was exactly  
143 equal to that at any other loci. Here we find that with reasonable amounts of variation among  
144 loci (e.g. in their expression level or the per-molecule damage from their misfolded form), the  
145 bistability disappears. Intermediate solutions evolve instead, where cryptic deleterious  
146 sequences are purged only in more highly expressed genes, and quality control evolves to  
147 intermediate levels. Variation among loci does not change the previous finding that evolvability  
148 tracks the proportion of loci that contain a benign rather than a deleterious cryptic sequence.

149  
150 The high rate of transcriptional error in *B. aphidicola* can be explained by adding a second bias  
151 toward deleterious mutations (in error rate), and hence a second drift barrier to our model. *B.*  
152 *aphidicola* and *E. coli* have high error rates for different reasons; high-fidelity quality control is  
153 redundant and unnecessarily expensive in *E. coli*, but unattainable in *B. aphidicola*, leading to  
154 similarly high transcriptional error rates.

155

## 156 METHODS

157 In the following sections, we describe the computational model used to simulate the evolution  
158 of different solutions to errors in gene expression. All simulations were run with Matlab  
159 (R2014a). Source code for the simulations is available at <https://github.com/MaselLab/>.

160

## 161 **Fitness**

162 We follow the additive model of Rajon and Masel (2011), as outlined below, with a few  
163 important modifications to accommodate variation in gene expression levels. The model's  
164 canonical example is the risk that a ribosome reads through a stop codon during translation.

165

166 The global mitigation strategy is to improve quality control of this gene expression subprocess.

167 We assume that additional quality control that reduces the error rate  $\rho$  by some proportion  
168 consumes a certain amount of time or comparable resource. Relative to a generation time of 1  
169 in the absence of quality control costs, this gives generation time  $1 + \delta \ln(1/\rho)$ , where  $\delta$  scales  
170 the amount of resources that could have been used in reproduction but are redistributed to  
171 quality control. Malthusian fitness is the inverse of generation time, giving

172

$$173 \quad w_{QC} = \frac{1}{1 + \delta \ln(1/\rho)} \quad (1)$$

174

175 Following Rajon and Masel (2011), we set  $\delta = 10^{-2.5}$ , such that reducing  $\rho$  from  $10^{-2}$  to  $10^{-3}$   
176 corresponds to a 0.7% reduction in fitness.

177

178 When a readthrough error happens, with frequency  $\rho$ , the consequences for fitness depend on  
179 the nature of the “cryptic sequence” that lies beyond the stop codon in the 3'UTR. The  
180 consequences of mistakes, mutational or otherwise, have a bimodal distribution, being either  
181 strongly deleterious (often lethal), or relatively benign, but rarely in between (Eyre-Walker and

182 Keightley 2007; Fudala and Korona 2009). For example, a strongly deleterious variant of a  
183 protein might misfold in a dangerous manner, while a benign variant might fold correctly,  
184 although with reduced activity. We assume that alternative alleles of “cryptic genetic  
185 sequences” can be categorized according to a benign/deleterious dichotomy.

186  
187 The local mitigation strategy, the alternative to global quality control, is thus for each cryptic  
188 sequence to evolve away from “deleterious” options and toward “benign” options. The local  
189 strategy of benign cryptic sequences has no direct fitness cost, but it is nevertheless difficult to  
190 evolve at so many loci at once. In contrast, expressing deleterious cryptic sequences has an  
191 appreciable cost. This cost scales both with the base rate of expression of the gene, and the  
192 proportion  $\rho$  of gene products that include the cryptic sequence.

193  
194 Let the expression of gene  $i$  be  $E_i$ . We assign the concentration  $E_i$  of protein molecules of type  $i$   
195 by sampling values of  $E_i$  from a  $\log_2$ -normal distribution with standard deviation  $\sigma_E$ . We define  $D$   
196 to be the total frequency of protein expression that would be highly deleterious if expressed in  
197 error:

198  
199 
$$D = \frac{\sum_{i \in \text{loci\_with\_del\_crypt\_seq}} E_i}{\sum_{i \in \text{loci}} E_i} \quad (2)$$

200  
201 where the numerator sums only over loci that are deleterious and the denominator sums over  
202 all loci. This normalization cancels out the effect of the mean value of  $E_i$ . We assume the costs of  
203 deleterious readthrough are additive across genes, based on the concept that misfolded proteins

204 (Thomas *et al.* 1995) may aggregate in a non-specific and harmful manner with other proteins  
205 and/or membranes (Kourie and Henry 2002), or may simply be expensive to dispose of (Goldberg  
206 2003). After the stop codon is read through, translation will usually end at a backup stop codon  
207 within the 3'UTR. Under the assumption of additivity, readthrough events will reduce fitness by  
208  $c\rho D$ , where  $c$  represents the strength of selection against misfolded proteins. Geiler-Samerotte  
209 *et al.* (2011) found that an increase in misfolded proteins of approximately 0.1% of total cellular  
210 protein molecules per cell imposed a cost of about 2% to relative growth rate. This gives an  
211 estimate of  $c = 0.02/0.1\% = 20$ .

212  
213 Readthrough involving benign cryptic sequences does not incur this cost. However, when all  
214 cryptic sequences are benign (i.e.  $D = 0$ ), nothing stops  $\rho$  from increasing to unreasonably large  
215 values, i.e.  $\rho > 0.5$ , which makes “erroneous” expression into the majority (and hence the “new  
216 normal”) form. To avoid this scenario, we add a cost in fitness  $c\rho^2(1-D)$ , whose impact is felt only  
217 at high values of  $\rho$ . One possible biological interpretation of this second order term is that with  
218 probability  $\rho^2$ , readthrough occurs not just through the regular stop codon, but also through the  
219 backup stop codon at the end of the benign cryptic genetic sequence. To reflect the effects of  
220 the double-error scenario under this interpretation, we therefore multiplied the second order  
221 term by the probability  $\mu_{del}/(\mu_{del}+\mu_{ben})$  that a neutrally evolving cryptic sequence will be  
222 deleterious, where  $\mu_{del}$  is the rate of deleterious-to-benign mutations and  $\mu_{ben}$  the reverse rate.  
223 Other double-error interpretations might involve different constants. In our case, the fitness  
224 component representing the cost of misfolded proteins is given by

225

$$226 \quad w_{\text{misfolding}} = \max(0, 1 - c\rho D - c\rho^2(1 - D) \frac{\mu_{\text{del}}}{\mu_{\text{del}} + \mu_{\text{ben}}}) \quad (3)$$

227

228 Eq. 3 is a natural extension of the additive model of Rajon and Masel (2011), generalizing to the  
229 case of variation in the degree of importance of cryptic loci. Where previous work referred to  
230 the number  $L_{\text{del}}$  of loci having the deleterious rather than benign form, we now distinguish  
231 between two measures,  $L_{\text{del}}$  and  $D$ , the latter reporting the proportion of gene product  
232 molecules rather than gene loci.

233

234 Rajon and Masel (2011) also obtained near-identical results using a very different, multiplicative  
235 model. While this suggests that the exact function form of Eq. 3 is unimportant, we chose the  
236 additive Eq. 3 model as the more reasonable of the two options. The multiplicative model is  
237 premised on loss-of-function of the wild-type proteins, which likely has negligible impact for  
238 small losses of a protein whose activity is already close to saturation. In contrast, the additive  
239 model is premised on gain-of-negative-function effects of misfolded proteins. These plausibly  
240 constitute a major burden on fitness, through a combination of toxicity, disposal costs, and  
241 resources spent to replace a faulty molecule with a normal one.

242

243 To study evolvability, let a subset of  $K$  (typically 50) out of the  $L$  (typically 600 or more) loci  
244 affect a quantitative trait  $x$ , selection on which creates a third fitness component. Error-free  
245 expression of locus  $k$ , occurring with frequency  $1-\rho$ , has quantitative effect  $\alpha_k$ , while expression  
246 that involves a benign version of the cryptic sequence has quantitative effect  $\alpha_k + \beta_k$ .  
247 Expression that involves a deleterious version of the cryptic sequence is assumed to result in a

248 misfolded protein that has no effect on the quantitative trait. We assume that expression level  
249  $E_k$  is constant and already factored into values of  $\alpha_k$  and  $\beta_k$ . This gives

250

$$251 \quad x = \sum_k^K ((1 - \rho)\alpha_k + \rho B_k(\alpha_k + \beta_k)) \quad (4)$$

252

253 where  $B_k = 1$  indicates a benign cryptic sequence and  $B = 0$  a deleterious one. As in Rajon and  
254 Masel (2011), we impose Gaussian selection on  $x$  relative to an optimal value  $x_{opt}$

255

$$256 \quad w_{trait}(x) = e^{\frac{-(x-x_{opt})^2}{2\sigma_f^2}} \quad (5)$$

257

258 where  $\sigma_f = 0.5$ .

259

260 Putting the three fitness components together, the relative fitness of a genotype is given by the  
261 product

262

$$263 \quad w = w_{QC} \times w_{misfolding} \times w_{trait}. \quad (6)$$

264

### 265 **Variance in expression levels**

266 We estimated the variance in expression  $\sigma_E^2$  from PaxDB (Wang *et al.* 2012; Wang *et al.* 2015),  
267 which is based on data released by the Global Proteome Machines (GMP) and other sources.

268 We inferred  $\sigma_E$  equal to 2.24 (based on GMP 2012 release) or 3.31 (GMP 2014 release), for *S.*

269 *cerevisiae*, and 2.93 (GMP 2014 release) for *S. pombe*. Note that while our quantitative

270 estimate of  $\sigma_E$  comes from variation in the expression levels of different proteins, consideration  
271 of variation along other lines might make a standard deviation of 2.25 into a conservative  
272 underestimate of the extent of variation. See Fig. S2 for an exploration of this parameter value.

273

## 274 **Mutation**

275 There are six kinds of mutation: 1) conversion of a deleterious cryptic sequence to a benign  
276 form, 2) conversion from benign to deleterious, 3) change to the error rate  $\rho$ , 4) change in the  $\alpha$   
277 value of one of the  $K$  quantitative trait genes, 5) change in the  $\beta$  value of one of those  $K$  genes,  
278 and 6) the co-option of a cryptic sequence to become constitutive, replacing the value of  
279 replacing  $\alpha_k$  with that of  $\alpha_k + \beta_k$  and re-initializing  $B_k$  and  $\beta_k$ .

280

281 It is this sixth kind of mutation that is responsible for the evolvability advantage of the local  
282 solution of benign cryptic sequences, providing more mutational raw material by which  $x$  might  
283 approach  $x_{opt}$  (Rajon and Masel 2011; Rajon and Masel 2013). The mutational co-option of a  
284 deleterious sequence ( $B = 0$ ) is too strongly deleterious to be favored, even when replacing  $\alpha_k$   
285 and  $\beta_k$  might be advantageous. In other words, only benign cryptic sequences are available for  
286 mutational co-option. We use the term co-option of a 3'UTR readthrough sequence to refer to  
287 the case when a stop codon is lost by mutation, and not just read through by the ribosome  
288 (Giacomelli *et al.* 2007; Vakhrusheva *et al.* 2011; Andreatta *et al.* 2015). Mutational co-option  
289 for mimicking the consequences of errors other than stop codon readthrough might involve  
290 mutations that change expression timing to make a rare protein-protein interaction common,  
291 or switch a protein's affinity preference between two alternative partners.

292  
293 Because we use an origin-fixation approach to simulate evolution (see below), only relative and  
294 not absolute mutation rates matter for our outcomes, with the absolute rates setting only the  
295 timescale – our rates are therefore effectively unitless. We use the same mutation rates as  
296 Rajon and Masel (2011), reduced ten-fold for convenience. Each locus with a benign cryptic  
297 sequence mutates to deleterious at rate  $\mu_{del} = 2.4 \times 10^{-8}$ , while deleterious loci mutate to benign  
298 less often, at rate  $\mu_{ben} = 6 \times 10^{-9}$ . Changes to the error rate  $\rho$  occur at rate  $\mu_{\rho} = 10^{-6}$ , while the  $\alpha$   
299 and  $\beta$  values of quantitative loci each change with rates  $\mu_{\alpha} = 3 \times 10^{-7}$  and  $\mu_{\beta} = 3 \times 10^{-8}$ ,  
300 respectively. Mutational co-option occurs at each quantitative locus at rate  $\mu_{coopt} = 2.56 \times 10^{-9}$ .  
301  
302 Each mutation to  $\rho$  increases  $\log_{10}\rho$  by an amount sampled from  $\text{Normal}(\rho_{bias}, \sigma_{\rho}^2)$ . By default,  
303 we set  $\rho_{bias} = 0$  and  $\sigma_{\rho} = 0.2$ . To study extremely small populations with drift barriers to evolving  
304 even a global solution, we set  $\rho_{bias} = 0.256$  and  $0.465$ , corresponding to ratios of  $\rho$ -increasing  
305 mutations:  $\rho$ -decreasing mutations of 9:1 and 99:1, respectively.  
306  
307 A similar scheme for  $\alpha$  and  $\beta$  might create, in the global solution case of relaxed selection, a  
308 probability distribution of  $\beta$  whose variance increases in an unbounded manner over time  
309 (Lande 1975; Lynch and Gabriel 1983). Following previous work (Rajon and Masel 2011; Rajon  
310 and Masel 2013), we therefore let mutations alter  $\alpha$  and  $\beta$  by an increment drawn from a  
311 normal distribution with mean  $-\alpha/a$  or  $-\beta/a$ , with  $a$  set to 750, and with standard deviation of  
312  $\sigma_m/K$  in both cases, with  $\sigma_m$  set to 0.5. In the case of neutrality, this mutational process



313 eventually reaches a stationary distribution with mean 0 and standard deviation as calculated in  
314 Eq. S3 of Rajon and Masel (2011):

315

$$316 \quad V(a, K, \sigma_m) = \frac{(\sigma_m/K)^2}{1 - ((a-1)/a)^2} \quad (7)$$

317

318 A co-option at gene  $k$  changes the gene's quantitative effect to

319

$$320 \quad (1 - \rho)(\alpha_k + \beta_k) + \rho B'_k(\alpha_k + \beta_k + \beta'_k) \quad (8)$$

321

322 where  $B'_k$  and  $\beta'_k$  are the state and the quantitative effect of a new cryptic sequence created by  
323 co-option. Following a co-option mutation at locus  $k$ , we set the new  $B_k$  equal to 1 or 0 with  
324 probabilities proportional to  $\mu_{ben}$  and  $\mu_{del}$ , and resample the value of  $\beta_k$  from Normal(0,  $V(a, K,$   
325  $\sigma_m)$ ).

326

### 327 **Evolutionary simulations by origin-fixation**

328 We model evolution using an approach known as “weak mutation” (Gillespie 1983), or “origin-  
329 fixation” (McCandlish and Stoltzfus 2014). This approximation of population genetics is accurate  
330 in the limit where the waiting time until the appearance of the next mutation destined to fix is  
331 substantially longer than its subsequent fixation time. The population can then be  
332 approximated as genetically homogeneous in any moment in time. While unrealistic for higher  
333 mutation rates and larger population sizes, origin-fixation models are computationally  
334 convenient. Still more importantly, origin-fixation models, unlike more realistic models with

335 segregating variation, allow the location of the drift barrier to be set externally in the form of  
336 the value of the parameter  $N$ , rather than having the location of the drift barrier emerge from  
337 complicated linkage phenomena within the model. Fortunately, for quantitative traits affected  
338 by multiple cryptic loci, most evolvability arises from diversity of the effects of co-option of  
339 different loci, rather than among the diversity of the effects of co-option from different starting  
340 genotypes (Rajon and Masel 2013). This allows us to study evolvability (in the population sense  
341 of Wagner (2008)) even in the absence of genetic diversity that is imposed by the origin-fixation  
342 formulation.

343  
344 Our computationally efficient implementation of origin-fixation dynamics is described in detail  
345 in the Supplement, simulating a series of mutations that successfully fix, and the waiting times  
346 between each.

347

### 348 **Initialization and convergence**

349 We initialized the trait optimum at  $x_{opt} = 0$ . We could have initialized all values of  $\alpha_k$  and  $\beta_k$  at  
350 zero. However, at steady state, variation in  $\sum_1^K \alpha_k$  and  $\sum_1^K \beta_k$  is far lower than would be  
351 expected from variation in  $\alpha_k$  and  $\beta_k$  – this emerges through a process of compensatory  
352 evolution (Rajon and Masel 2013). Allowing a realistic steady state to emerge in this way is  
353 computationally slow under origin-fixation dynamics, especially when  $N$  is large. We instead  
354 sampled the initial values of  $\alpha_k$  and  $\beta_k$  from  $\text{Normal}(0, V(a, K, \sigma_m))$ , where  $V(a, K, \sigma_m)$  is defined  
355 by Eq. 7, and then subtracted  $\bar{\alpha}$  from  $\alpha_k$  and  $\bar{\beta}$  from  $\beta_k$ , where  $\bar{\alpha}$  and  $\bar{\beta}$  are the means of a  
356 genotype across each of its quantitative loci  $k$ . This process initializes  $\alpha_k$  and  $\beta_k$  to have

357 variances equal to those of the stationary distributions, while the overall trait value is initialized  
358 at the optimal value, zero. This procedure greatly reduces the burn-in computation time  
359 needed to achieve a somewhat subtle state of negative within-genotype among-loci  
360 correlations. We confirmed that subsequent convergence of the variance of  $\sum_1^K \alpha_k$  was fast,  
361 occurring in less than 1000 steps, where a “step” is defined to be the fixation of one mutation.  
362 We expect  $\log_{10}\rho$ ,  $D$ , and variation in  $\beta_k$  to converge even faster than variation in  $\alpha_k$ .

363

364 For the low- $\rho$  initial conditions,  $\rho$  was initialized at  $10^{-5}$ , and we initialized the benign vs.  
365 deleterious status of cryptic sequences at the neutral mutational equilibrium, choosing exactly  
366  $L \times \mu_{del} / (\mu_{del} + \mu_{ben})$  (rounded to the nearest integer) to be deleterious, independently of their  
367 different values of  $E$ . For the high- $\rho$  initial conditions, we set  $\rho$  to  $10^{-1}$ , and made all cryptic  
368 sequences benign.

369

370 We ran simulations for  $10^5$  steps, recording information at fixed times (measured in terms of  
371 waiting times), corresponding to approximately every 1000 steps on average, and hence  
372 yielding about 100 timepoints. To summarize the evolutionary outcome, we calculated the  
373 arithmetic means of  $\log_{10}\rho$ , of  $L_{del}$ , and of  $D$  among the last 20 timepoints, i.e. approximating  
374 steps  $0.8 \times 10^5 - 1 \times 10^5$ .

375

### 376 **Evolvability**

377 After adaptation to a trait optimum of  $x_{opt} = 0$  had run to convergence (i.e. after  $10^5$  steps), we  
378 changed  $x_{opt}$  to 2, forcing the quantitative trait to evolve rapidly. This allows the co-option of

379 benign cryptic sequences an opportunity to increase evolvability. We measured evolvability in  
380 two ways: as the inverse of the waiting time before trait  $x$  exceeded 1, and the inverse of the  
381 waiting time before the population recovered half of the fitness it lost after  $x_{opt}$  changed. By  
382 default, we present results showing evolvability as time to fitness recovery; evolvability as time  
383 to trait recovery is shown only in Fig. S3.

384  
385 We want our measures of evolvability to reflect a genotype's potential to generate beneficial  
386 mutations, but this goal was complicated by population size. A large population finds a given  
387 beneficial mutation faster than a small population does, inflating the total fixation flux  
388  $\sum_{i \in \text{beneficial\_mutation}} \mu_i N P_{fix}(i)$ , where  $\mu_i N$  is the influx of mutations of beneficial type  $i$  and  
389  $P_{fix}$  is their probability of fixation (the latter described by Eq. 9 in the supplemental material), in  
390 direct proportion to population size. We therefore divided our evolvability measures by the  
391 population size to correct for this effect. This normalization converts the population-level  
392 evolvability measure into a measure of the population-size-independent evolvability of a single  
393 individual that has the genotype of interest.

394

## 395 RESULTS

396 Recall that in the absence of variation in expression among genes, there are two solutions to  
397 handle erroneous expression due to stop codon readthrough: at high population size  $N$ , the  
398 local solution purges all deleterious cryptic sequences, making high rates of readthrough  
399 harmless, while at low  $N$ , the global solution reduces the rate of readthrough, allowing  
400 deleterious cryptic sequences to accumulate near-neutrally. At intermediate  $N$ , we see

401 bistability, with either solution possible, depending on starting conditions (Fig. 1,  $\sigma_E = 0$ ). It is  
402 important to note that we use the word “bistability” loosely. Strictly speaking, bistability means  
403 that the system has two stable steady states (here a state is defined by readthrough rate and  
404 the exact property of each cryptic sequence), i.e. two attractors. But in a stochastic model,  
405 there are no attractors in the strict sense of the word, only a stationary distribution of states.  
406 We use the term bistability to refer to the case where the stationary distributions of states has  
407 two modes. Transitions between the two modes are rare, therefore the two modes can be  
408 loosely interpreted as the two attractors of the system.

409  
410 Our results qualitatively reproduce the bistability reported by Rajon and Masel (2011) for the  
411 case where there is no expression variation among genes, though the range of values of  $N$   
412 leading to bistability is smaller than that found in Rajon and Masel (2011) in which a full Wright-  
413 Fisher simulation is used. The smaller range of bistability in our model could be caused by the  
414 ease with which long-term evolution is captured using an origin-fixation framework, or by other  
415 subtle differences between the approaches, e.g. the greater ease of compensatory evolution  
416 under Wright-Fisher dynamics than under origin-fixation. We chose origin-fixation mainly to  
417 reduce the computational burden, which for our study was increased by the need to track  
418 individual loci, in contrast to previous work that needed only to track the number of loci with  
419 deleterious cryptic sequence, without distinguishing their identities (Rajon and Masel 2011;  
420 Rajon and Masel 2013).

421

422 However, bistability vanishes with variation in expression among genes (Fig. 1,  $\sigma_E = 2.25$  and  $\sigma_E$   
423  $= 3.5$ ). To understand why, consider a population initialized at low readthrough rate ( $\rho$ ) and many  
424 deleterious cryptic sequences. Because the strength of selection against a deleterious cryptic  
425 sequence at locus  $i$  is proportional to  $\rho E_i$  (the effect of a locus  $i$  on  $D$  in Eq. 3 is proportional to  
426  $E_i$ ), purging works at the most highly expressed loci, even when  $\rho$  is low. This lowers the  
427 proportion  $D$  of readthrough events that are deleterious, which relaxes selection for high fidelity,  
428 leading to an increase in  $\rho$ . As  $\rho$  increases, loci with lower  $E_i$  become subject to effective purging,  
429 which further reduces  $D$ , which feeds back to increase  $\rho$  further. Because  $E_i$  is log-normally  
430 distributed, but contributes linearly to selection via  $D$ , each round of the feedback loop involves  
431 smaller changes than the last. Eventually, the changes are too small for selection on them to  
432 overcome mutation bias in favor of deleterious sequences. Similarly, when a population is  
433 initialized at high  $\rho$ , mutational degradation begins at low  $E_i$  sites and arrests when selection is  
434 strong enough to kick in. The point of balance between mutation bias and selection defines a  
435 single intermediate attractor for  $\sigma_E \geq 2.25$ , instead of the bistable pair of attractors found for  
436 uniform  $E_i$  ( $\sigma_E = 0$ ). For  $\sigma_E < 2.25$ , bistability is still found, but for a narrower range of population  
437 sizes than in the absence of variation (Fig. S2).

438  
439 Even though bistability is not found for  $\sigma_E = 2.25$ , there is still a fairly sharp dichotomy, with  
440 solutions being either local (high  $\rho$  and low  $L_{del}$ ) or global (low  $\rho$  and high  $L_{del}$ ), and intermediate  
441 solutions found only for a very restrictive range of  $N$ , following a sigmoidal curve (Fig. 1a and 1c).  
442 Increasing variation in expression among genes blurs the boundary between the local solution  
443 and the global solution. Intermediate solutions are found for broader ranges of  $N$  as expression

444 variance  $\sigma_E$  increases to 3.5. The trend, as expression variance  $\sigma_E$  increases from 0, is to first  
445 replace bistability with a limited range of intermediate solutions ( $\sigma_E = 2.25$ ), and then for the  
446 intermediate solutions to become more prevalent, with extreme local and global solutions  
447 becoming less attainable as  $\sigma_E > 2.25$ .

448  
449 The breakdown of the local solution begins with intermediate values of  $L_{del}$ , while the breakdown  
450 of the global solution begins with intermediate values of  $\rho$  and  $D$  (Fig. 1 a-c). The breakdown of  
451 global solutions involves high-expression loci (Fig. 2), which affect  $D$  more than  $L_{del}$ . In contrast,  
452 the breakdown of local solutions involves low-expression loci (Fig. 2), which affect  $L_{del}$  more than  
453  $D$ . Because  $\rho$  is better described as co-evolving with  $D$  than with  $L_{del}$ , as explained earlier,  
454 intermediate values of  $\rho$  are seen more in the breakdown of global than local solutions.

455  
456 A primary motivation behind characterizing the two solutions is that the local solution was found  
457 to have dramatically higher evolvability than the global solution (Rajon and Masel 2011). We  
458 therefore check whether this conclusion still broadly stands in the presence of variance in  
459 expression levels. The local solution promotes evolvability by making benign cryptic sequences  
460 available for co-option. Differences in evolvability between genotypes should therefore be  
461 largely determined by the fraction of quantitative trait loci that carry benign rather than  
462 deleterious cryptic sequences. In agreement with this, evolvability inversely mirrors  $L_{del}$ , as a  
463 function of population size, i.e., evolvability (Fig. 1d) resembles  $L_{del}$  (Fig. 1c) far more than it  
464 resembles  $\rho$  (Fig. 1a) or  $D$  (Fig. 1b).

465

466 The distinction between global and local solutions becomes more extreme when the mutation  
467 bias toward deleterious rather than benign cryptic sequences is increased from 4:1 ratio to a 99:1  
468 ratio, but persists even when the mutation bias is eliminated in favor of a 1:1 ratio (Fig. 3). In the  
469 absence of mutation bias, there is less evolvability to be gained by the local relative to the global  
470 solution, since half the quantitative loci are available for co-option regardless (Fig. 3c).  
471 Nevertheless, a small evolvability advantage to the local solution can still be observed (Fig. 3d).  
472 In any case, assuming mutation bias toward deleterious options is biologically reasonable, and  
473 Fig. 3 shows that results are not sensitive to the quantitative strength of our assumption on this  
474 count.

475  
476 When we also account for mutation bias that tends to increase rather than decrease the error  
477 rate  $\rho$ , our model can explain the previously puzzling observation that the rate of  
478 transcriptional errors in small- $N_e$  endosymbiont bacteria *Buchnera* is so much higher than that  
479 of *C. elegans*, and almost as high as that of large- $N_e$  *E. coli* (McCandlish and Plotkin 2016;  
480 Traverse and Ochman 2016b). In extremely small populations, even the global solution is  
481 subject to a drift barrier, making  $\rho$  higher than its optimal value. For  $N$  so small such that most  
482  $\rho$ -increasing mutations pass through the drift barrier,  $\rho$  can be almost as large as that in large  
483 populations (Fig. 4a). Despite their high error rates, these extremely small populations also  
484 carry heavy loads of deleterious cryptic products (Fig. 4b and c), consistent with the fact that in  
485 *B. aphidicola*, unlike *E. coli*, selection is unable to reduce the fraction of non-synonymous  
486 transcriptional errors that are non-synonymous (Traverse and Ochman 2016a). High  $\rho$  shows  
487 the absence of a global solution, while high  $D$  and  $L_{del}$  show the absence of a local solution;



488 neither solution is found for a sufficiently small population. Similar error rates in large and small  
489 populations can also be found, given bias in mutations to  $\rho$ , when there is no variation in  
490 expression levels (Fig. S5).

491  
492 The parameters in our model can be classified into three groups, and the exploration of their  
493 values is summarized in Table S1. The first group controls selection coefficients relevant to the  
494 global vs. local solution outcome: the variance in expression levels ( $\sigma_{\epsilon}^2$ ), the number of loci ( $L$ ,  
495 Fig. S4), the cost of misfolded protein molecules ( $c$ ), and the cost of quality control ( $\delta$ , Fig. S6).  
496 The second group controls mutation bias relevant to the global vs. local solution outcome: the  
497 frequency with which mutations turn deleterious cryptic sequences benign versus the reverse  
498 ( $\mu_{ben}:\mu_{del}$ ), whether mutations to  $\rho$  tend to increase or decrease it ( $P_{+\rho}:P_{-\rho}$ ), and variance in the  
499 magnitude of mutations to  $\rho$  ( $\sigma_{\rho}^2$ , Fig. S7). The third group contains all the parameters that  
500 control the evolution of quantitative traits encoded by a minority of loci relevant to the  
501 evolvability properties. Because our focus in this manuscript is on the evolution of global vs.  
502 local solutions, not on the precise details of the relationship between local solutions and  
503 evolvability, these parameter values were explored less.

504  
505 The influence of  $\sigma_{\epsilon}^2$  dominates our results. Its effect in eliminating bistability holds, with the  
506 one exception that very “cheap” quality control could partially restore bistability (Fig. S6).  
507 Otherwise, we found that three parameters –  $c$ ,  $\delta$ , and  $\mu_{ben}:\mu_{del}$  – are the main determinants of  
508 the population size at which the transition between global and local solutions takes place, and  
509 of the exact error rate that evolves for global and local solutions (Table S1). The other

510 parameters in the first and second groups have little or no influence on the evolutionary  
511 outcomes that we study. In general, parameters in the first group, controlling selection, have  
512 stronger effects than the second group, controlling mutation bias.

513

## 514 DISCUSSION

515 When genes vary in their expression levels, the dichotomy between the local and global  
516 solutions is replaced by a continuous transition. Very large populations still resemble the local  
517 solution, although mutations making cryptic sequences deleterious still pass through the drift  
518 barrier in the occasional low-expression gene. Very small populations still resemble the global  
519 solution, although mutations making cryptic sequences deleterious may still be effectively  
520 purged in a few high-expression genes; because their high expression disproportionately affects  
521 the burden from misexpression, this relaxes expression for high fidelity, leading to less strict  
522 quality control.

523

524 In agreement with drift barrier theory, large- $N_e$  *E. coli* exhibits a local solution – a tendency for  
525 transcription errors to have synonymous effects – while small- $N_e$  *B. aphidicola* does not  
526 (Traverse and Ochman 2016a). While as predicted, the global solution of low transcriptional  
527 error rates does not obey the naïve drift barrier expectation of being higher in *B. aphidicola*  
528 than in *E. coli* (Traverse and Ochman 2016a), nor are transcription error rates drastically lower  
529 in *B. aphidicola* as predicted by previous theory on the interplay between global and local  
530 solutions (Rajon and Masel 2011; McCandlish and Plotkin 2016). This significantly lower rate  
531 relative to *E. coli* is, however, found in intermediate- $N_e$  *C. elegans*. Where previous work (Rajon

532 and Masel 2011) explained only the relative rates for *E. coli* and *C. elegans*, here we also explain  
533 the high error rate of *B. aphidicola* by taking into account a drift barrier on the global solution  
534 of low error rates. This drift barrier is significant because of mutation bias towards higher error  
535 rates. Small *B. aphidicola* populations have higher error rates than *C. elegans* because it is the  
536 best that evolution at low  $N_e$  can manage, despite the deleterious consequences; large *E. coli*  
537 populations have similarly high error rates because with the worst consequences of error  
538 already purged, they don't need to incur the cost that quality control entails.

539  
540 With small amounts of variation in expression among genes, the range of intermediate values  
541 of  $N_e$  for which bistability is found shrinks. With more variation, bistability vanishes in favor of a  
542 sigmoidal transition between global and local solutions. With still more, the sigmoid is  
543 smoothed out, and intermediate solutions are found for most values of  $N_e$ .

544  
545 To interpret our results correctly, we must therefore estimate the degree to which genes vary.  
546 The results presented here focus on two estimates of the variation in log-expression in yeast,  
547 namely standard deviations of 2.25 and 3.5. However, variation among genes in the deleterious  
548 consequences of misfolding, in addition to variation in expression levels, might make larger  
549 standard deviations a better model of reality, further supporting a continuum of intermediate  
550 solutions. In other words, the value of  $c$  in Eq. 3 may vary among genes. Note that apart from  
551 the second-order  $\rho^2$  term, the cost of a deleterious misfolded protein  $i$  depends only on the  
552 product of  $c_i$  and expression level  $E_i$ . Given log-normal distributions of  $c_i$  and expression level  
553  $E_i$ , the variance of the log-product is equal to the sum of the two log-variances, so we can

554 transform this scenario into one where  $c$  is constant, and  $\sigma_{E^2}$  is equal to this sum. This can be  
555 done because changing  $c_i$  and  $E_i$  only affects  $w_{misfolding}$  and not other factors such as the  
556 magnitude of a locus's influence on the quantitative trait. In other words, adding variation to  $c$   
557 is almost equivalent to increasing the variance in expression levels.

558  
559 The values of  $\mu_{del}$  and  $\mu_{ben}$  may also vary among genes. Drift barrier effects operate via the  
560 effect of population size on the fate of deleterious not beneficial mutations – if purging is  
561 efficient, then the beneficial mutation rate does not matter, because a single beneficial  
562 mutation is enough. We therefore focus on  $\mu_{del}$ . The inclusion of a benign-to-deleterious  
563 mutation  $M_i$  at locus  $i$  depends on the product of  $\mu_{del}$  at locus  $i$  and  $M_i$ 's probability of fixation.  
564 It seems likely that variation among genes in the probability that a deleterious cryptic sequence  
565 becomes fixed will swamp variation in the deleterious mutation rate – variation in expression  
566 levels cause the former to vary over orders of magnitude. Note that as for the case of variation  
567 in  $c$ , it is possible to construct a manipulation of  $E_i$  that has the same effect on the relevant  
568 product, via the probability of fixation, as would occur given a change in  $\mu_{del}$ . While this case is  
569 less neat than for the product  $c_i E_i$ , it illustrates that a model of variation in expression levels  
570 can reflect, to some extent, the effect of variation in  $\mu_{del}$ .

571  
572 Our model makes three critical assumptions, which must be understood for the results to be  
573 interpreted appropriately. First, a “locus” in our model consists of one regular and one cryptic  
574 sequence. The primary example that we used to parameterize the simulations posits an entire  
575 protein-coding gene as the regular sequence, and the extended polypeptide resulting from stop

576 codon readthrough as the cryptic alternative. In the example of transcriptional errors, a locus is  
577 a single codon, with its corresponding amino acid being the regular sequence, and the most  
578 common consequence of a transcriptional error as the cryptic. The case of one regular  
579 sequence and many alternative cryptic ones has not been modeled. Similarly, proteins may  
580 each have a regular fold or binding partner, and our model considers the contrast between this  
581 state and a single cryptic alternative.

582  
583 Second, we assume that the rate of gene expression errors is set globally, across all loci. In  
584 reality, individual context may also affect the error rate, giving error rates a local solution  
585 aspect as well. A model of three rather than two interacting solutions – global error rates, local  
586 error rates, and local robustness to the consequences of error – remains for future work.  
587 Perhaps highly expressed genes will have both more benign cryptic sequences and lower rates  
588 of error, or perhaps the evolution of one kind of local solution will alleviate the need for  
589 another. Testing this empirically requires data on site-specific error rates and on a credible  
590 marker for the benign status of members of an identifiable class of cryptic sequences. Such  
591 tools are now becoming available, and indeed we recently found a positive correlation between  
592 a large number of readthrough errors at a particular stop codon and the benign status of the  
593 readthrough translation product (Kosinski et al., manuscript in preparation). We also reanalyzed  
594 the data of Traverse and Ochman (2016a) to find that highly expressed transcripts have lower  
595 transcriptional error rates (unpublished result).

596

597 Finally, we assume that the consequences of errors have a bimodal distribution: either highly  
598 deleterious or largely benign, but rarely in between. In other words, we assume that a basic  
599 phenomenon in biology is that changes tend to either break something, or to tinker with it.  
600 There are a variety of lines of evidence supporting this intuitively reasonable assumption  
601 (Fudala and Korona 2009; Wylie and Shakhnovich 2011).

602

603

#### ACKNOWLEDGEMENTS

604 This work was supported by the John Templeton Foundation [grant number 39667]. DJP was  
605 also funded by the Undergraduate Biology Research Program at the University of Arizona. We  
606 thank Lilach Hadany, Yoav Ram, and other members of the Hadany group for helpful  
607 discussions that prompted us to explore variation in expression. We thank Paul Nelson for  
608 developing the idea of local error rates as an expansion of our model, Ben Wilson for help with  
609 R, and Etienne Rajon, Yoav Ram, Tobias Warnecke, and one anonymous reviewer for helpful  
610 comments on the manuscript. We also thank Charles Traverse and Howard Ochman for sharing  
611 their data on transcriptional errors. An allocation of computer time from the UA Research  
612 Computing High Performance Computing (HPC) and High Throughput Computing (HTC) at the  
613 University of Arizona is gratefully acknowledged.

614

#### LITERATURE CITED

615 Adachi, M., and A. R. O. Cavalcanti, 2009 Tandem Stop Codons in Ciliates That Reassign Stop  
616 Codons. *J. Mol. Evol.* 68: 424-431.

- 617 Andreatta, M. E., J. A. Levine, S. G. Foy, L. D. Guzman, L. J. Kosinski *et al.*, 2015 The Recent De  
618 Novo Origin of Protein C-Termini. *Genome Biology and Evolution* 7: 1686-1701.
- 619 Brettner, L. M., and J. Masel, 2012 Protein stickiness, rather than number of functional protein-  
620 protein interactions, predicts expression noise and plasticity in yeast. *BMC Systems*  
621 *Biology* 6: 128.
- 622 Drummond, D. A., and C. O. Wilke, 2008 Mistranslation-Induced Protein Misfolding as a  
623 Dominant Constraint on Coding-Sequence Evolution. *Cell* 134: 341-352.
- 624 Eyre-Walker, A., and P. D. Keightley, 2007 The distribution of fitness effects of new mutations.  
625 *Nat. Rev. Genet.* 8: 610-618.
- 626 Frank, S. A., 2007 Maladaptation and the Paradox of Robustness in Evolution. *PLoS ONE* 2:  
627 e1021.
- 628 Fudala, A., and R. Korona, 2009 Low frequency of mutations with strongly deleterious but  
629 nonlethal fitness effects. *Evolution* 63: 2164-2171.
- 630 Geiler-Samerotte, K. A., M. F. Dion, B. A. Budnik, S. M. Wang, D. L. Hartl *et al.*, 2011 Misfolded  
631 proteins impose a dosage-dependent fitness cost and trigger a cytosolic unfolded  
632 protein response in yeast. *Proc. Natl. Acad. Sci. U.S.A.* 108: 680-685.
- 633 Giacomelli, M. G., A. S. Hancock and J. Masel, 2007 The conversion of 3' UTRs into coding  
634 regions. *Mol. Biol. Evol.* 24: 457-464.
- 635 Gillespie, J. H., 1983 Some properties of finite populations experiencing strong selection and  
636 weak mutation. *Am. Nat.* 121: 691-708.
- 637 Goldberg, A. L., 2003 Protein degradation and protection against misfolded or damaged  
638 proteins. *Nature* 426: 895-899.

- 639 Good, B. H., and M. M. Desai, 2014 Deleterious Passengers in Adapting Populations. *Genetics*  
640 198: 1183-1208.
- 641 Gout, J.-F., W. K. Thomas, Z. Smith, K. Okamoto and M. Lynch, 2013 Large-scale detection of in  
642 vivo transcription errors. *Proc. Natl. Acad. Sci. U.S.A.* 110: 18584-18589.
- 643 Haldane, J. B. S., 1957 The cost of natural selection. *J. Genetic.* 55: 511-524.
- 644 Kourie, J. I., and C. L. Henry, 2002 Ion channel formation and membrane-linked pathologies of  
645 misfolded hydrophobic proteins: The role of dangerous unchaperoned molecules. *Clin.*  
646 *Exp. Pharmacol. Physiol.* 29: 741-753.
- 647 Krakauer, D. C., and J. B. Plotkin, 2002 Redundancy, antiredundancy, and the robustness of  
648 genomes. *Proc. Natl. Acad. Sci. U.S.A.* 99: 1405-1409.
- 649 Lande, R., 1975 The maintenance of genetic variability by mutation in a polygenic character  
650 with linked loci. *Genet. Res.* 26: 221-235.
- 651 Liang, H., A. R. O. Cavalcanti and L. F. Landweber, 2005 Conservation of tandem stop codons in  
652 yeasts. *Genome Biol.* 6: R31.
- 653 Lynch, M., 2007 *The origins of genome architecture*. Sinauer Associates, Sunderland.
- 654 Lynch, M., 2010 Evolution of the mutation rate. *Trends Genet.* 26: 345-352.
- 655 Lynch, M., 2012 Evolutionary layering and the limits to cellular perfection. *Proc. Natl. Acad. Sci.*  
656 *U.S.A.* 109: 18851-18856.
- 657 Lynch, M., and W. Gabriel, 1983 Phenotypic evolution and parthenogenesis. *Am. Nat.* 122: 745-  
658 764.
- 659 McCandlish, D. M., and J. B. Plotkin, 2016 Transcriptional errors and the drift barrier. *Proc. Natl.*  
660 *Acad. Sci. U.S.A.* 113 136-3138



- 661 McCandlish, D. M., and A. Stoltzfus, 2014 Modeling Evolution Using the Probability of Fixation:  
662 History and Implications. *Q. Rev. Biol.* 89: 225-252.
- 663 Mira, A., and N. A. Moran, 2002 Estimating Population Size and Transmission Bottlenecks in  
664 Maternally Transmitted Endosymbiotic Bacteria. *Microbial Ecology* 44: 137-143.
- 665 Nichols, J. L., 1970 Nucleotide Sequence from the Polypeptide Chain Termination Region of the  
666 Coat Protein Cistron in Bacteriophage R17 RNA. *Nature* 225: 147-151.
- 667 Rajon, E., and J. Masel, 2011 The evolution of molecular error rates and the consequences for  
668 evolvability. *Proc. Natl. Acad. Sci. U.S.A.* 108: 1082-1087.
- 669 Rajon, E., and J. Masel, 2013 Compensatory Evolution and the Origins of Innovations. *Genetics*  
670 193: 1209-1220.
- 671 Rispe, C., F. Delmotte, R. C. H. J. van Ham and A. Moya, 2004 Mutational and Selective  
672 Pressures on Codon and Amino Acid Usage in *Buchnera*, Endosymbiotic Bacteria of  
673 Aphids. *Genome Res.* 14: 44-53.
- 674 Thomas, P. J., B.-H. Qu and P. L. Pedersen, 1995 Defective protein folding as a basis of human  
675 disease. *Trends Biochem. Sci.* 20: 456-459.
- 676 Traverse, C. C., and H. Ochman, 2016a Conserved rates and patterns of transcription errors  
677 across bacterial growth states and lifestyles. *Proc. Natl. Acad. Sci. U.S.A.* 113: 3311-3316
- 678 Traverse, C. C., and H. Ochman, 2016b Correction for Traverse and Ochman, Conserved rates  
679 and patterns of transcription errors across bacterial growth states and lifestyles. *Proc.*  
680 *Natl. Acad. Sci. U.S.A.* 113: E4257-E4258.
- 681 Vakhrusheva, A., M. Kazanov, A. Mironov and G. Bazykin, 2011 Evolution of Prokaryotic Genes  
682 by Shift of Stop Codons. *J. Mol. Evol.* 72: 138-146.

- 683 Wagner, A., 2008 Robustness and evolvability: a paradox resolved. Proc. R. Soc. Lond. Ser. B-  
684 Biol. Sci. 275: 91-100.
- 685 Wang, M., C. J. Herrmann, M. Simonovic, D. Szklarczyk and C. von Mering, 2015 Version 4.0 of  
686 PaxDb: Protein abundance data, integrated across model organisms, tissues, and cell-  
687 lines. Proteomics 15: 3163-3168.
- 688 Wang, M., M. Weiss, M. Simonovic, G. Haertinger, S. P. Schimpf *et al.*, 2012 PaxDb, a Database  
689 of Protein Abundance Averages Across All Three Domains of Life. Mol. Cell. Proteomics  
690 11: 492-500.
- 691 Warnecke, T., and L. D. Hurst, 2011 Error prevention and mitigation as forces in the evolution of  
692 genes and genomes. Nat Rev Genet 12: 875-881.
- 693 Williams, I., J. Richardson, A. Starkey and I. Stansfield, 2004 Genome-wide prediction of stop  
694 codon readthrough during translation in the yeast *Saccharomyces cerevisiae*. Nucleic  
695 Acids Res. 32: 6605-6616.
- 696 Wu, X., and L. D. Hurst, 2015 Why Selection Might Be Stronger When Populations Are Small:  
697 Intron Size and Density Predict within and between-Species Usage of Exonic Splice  
698 Associated cis-Motifs. Mol. Biol. Evol. 32: 1847-1861.
- 699 Wylie, C. S., and E. I. Shakhnovich, 2011 A biophysical protein folding model accounts for most  
700 mutational fitness effects in viruses. Proc. Natl. Acad. Sci. U.S.A. 108: 9916-9921.

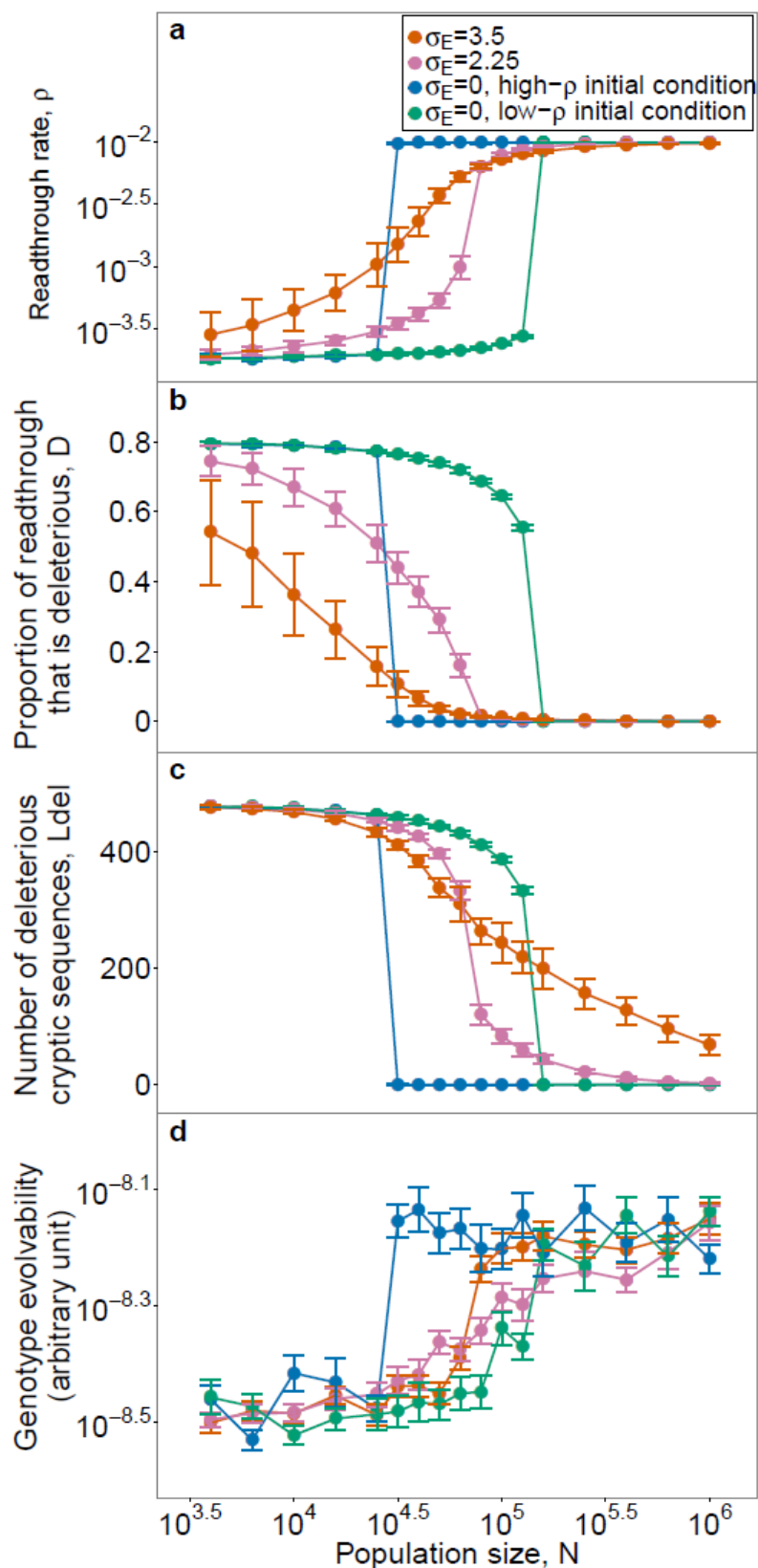


**Figure 1:** Evolutionary dynamics are bistable in the absence of variation in gene expression ( $\sigma_E = 0$ ), but not with variation in gene expression ( $\sigma_E = 2.25$  and  $\sigma_E = 3.5$ ). We calculated the average values of  $\rho$ ,  $D$ , and  $L_{del}$  towards the end of the simulations, and then measured the genotype evolvability after changing the optimal trait value (see Methods for details). For each value of  $N$ , 20 simulations were initialized at high- $\rho$  conditions and 15 at low- $\rho$  conditions. For  $\sigma_E = 2.25$  and  $\sigma_E = 3.5$ , simulations from the two initial conditions reached indistinguishable endpoints (Fig. S1), so the results were pooled. The increment in  $N$  is  $10^{0.1}$  between  $10^{4.4}$  and  $10^{5.2}$  to increase resolution, and is  $10^{0.2}$  elsewhere. At  $\sigma_E = 0$ ,  $D$  is indistinguishable from zero for  $N \geq 10^{5.2}$  under high- $\rho$  conditions and for  $N \geq 10^{4.7}$  under low- $\rho$  conditions, corresponding to  $L_{del}$  being effectively zero. In contrast, when  $\sigma_E = 2.25$  or  $3.5$ , because the weakness of selection on low-expression genes prevents  $L_{del}$  from falling all the way to zero,  $D$  never quite reaches zero either, despite appearing superimposable in **b**. For **a** to **c**, data is shown as mean  $\pm$  SD. For evolvability (**d**), data is shown as mean  $\pm$  SE. For **a** and **d**, these apply to log-transformed values. Evolvability is based on time to fitness recovery; see Fig. S3 for similar results based on time to trait recovery.  $L = 600$ .

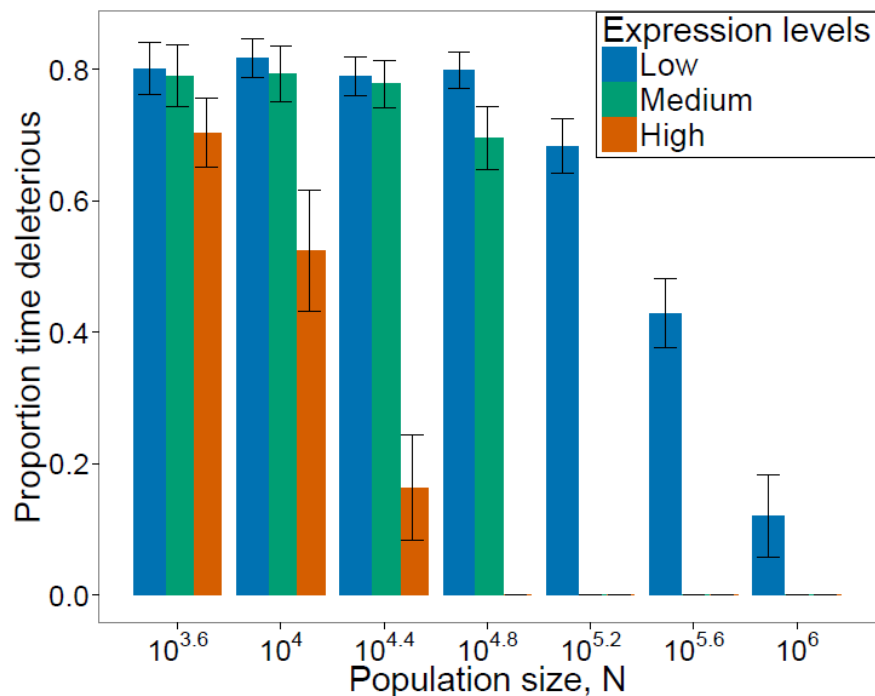


**Figure 2:** The effectiveness of purging a cryptic sequence of deleterious mutations depends on its expression level. We examined the states of the cryptic sequences of the loci with the 10 highest, the 10 lowest, and the 10 median expression levels among the 600 loci in each of the simulations showed in Fig. 1 ( $\sigma_E = 2.25$ ). We counted how often each locus contained a deleterious cryptic sequence among the last 20 timepoints we had collected from that simulation. Bars represent the proportion of time that each of the 10 loci carried a deleterious cryptic sequence, averaged over 20 replicates, and shown as  $\text{mean} \pm \text{SD}$ . Simulations were initialized at low- $p$  conditions.

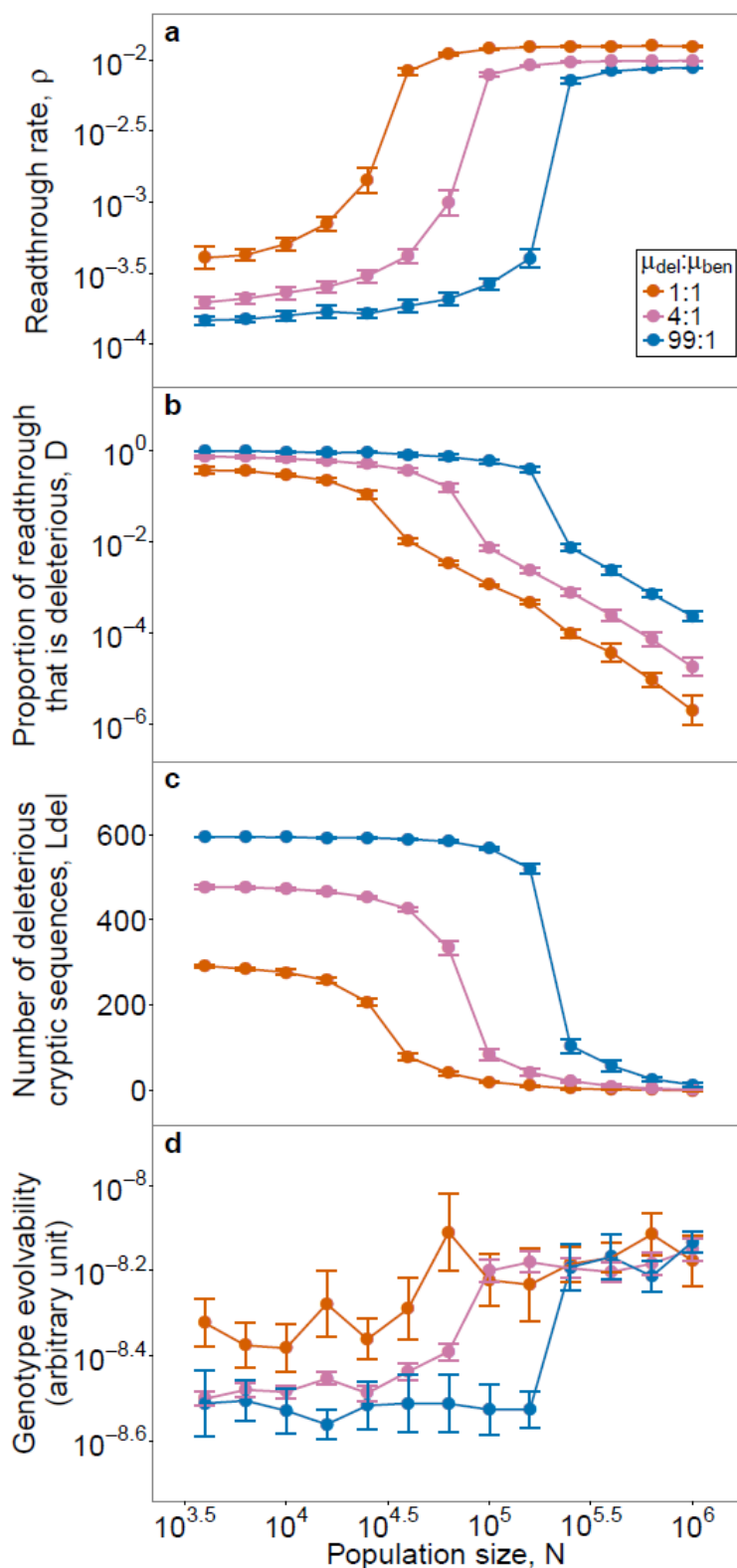


**Figure 3:** Results become more extreme when the mutation bias in the state of a cryptic sequence is increased from 4:1 ratio to a 99:1 ratio, but do not disappear completely when the mutation bias is eliminated in favor of a 1:1 ratio. The location of the drift barrier shifts as a function of mutation bias, but the dichotomy between local and global solutions (as seen in values of  $\rho$  and  $D$ ) is not sensitive to relaxing the mutation bias. The advantage of the local solution with respect to evolvability (as seen in **d** and mirrored in  $L_{del}$  (**c**)) is more sensitive to lack of mutation bias, but is still visible even with a 1:1 ratio. To compare results across different mutation biases, we kept the sum of the two mutation rates constant. For the low- $\rho$  initial conditions, the number of deleterious cryptic sequences was initialized at the neutral mutational equilibrium of  $L \times \mu_{del} / (\mu_{del} + \mu_{ben})$  (rounded to the nearest integer). For  $\mu_{del} : \mu_{ben} = 4:1$ , we reused the results shown in Fig. 1. For the other ratios, five replicates were run for each

initial condition, and pooled. For panels **a** to **c**, data is shown as mean  $\pm$  SD. For panel **d**, data is shown as mean  $\pm$  SE. For **a** and **d**, these apply to log-transformed values.  $L = 600$  and  $\sigma_E = 2.25$ .

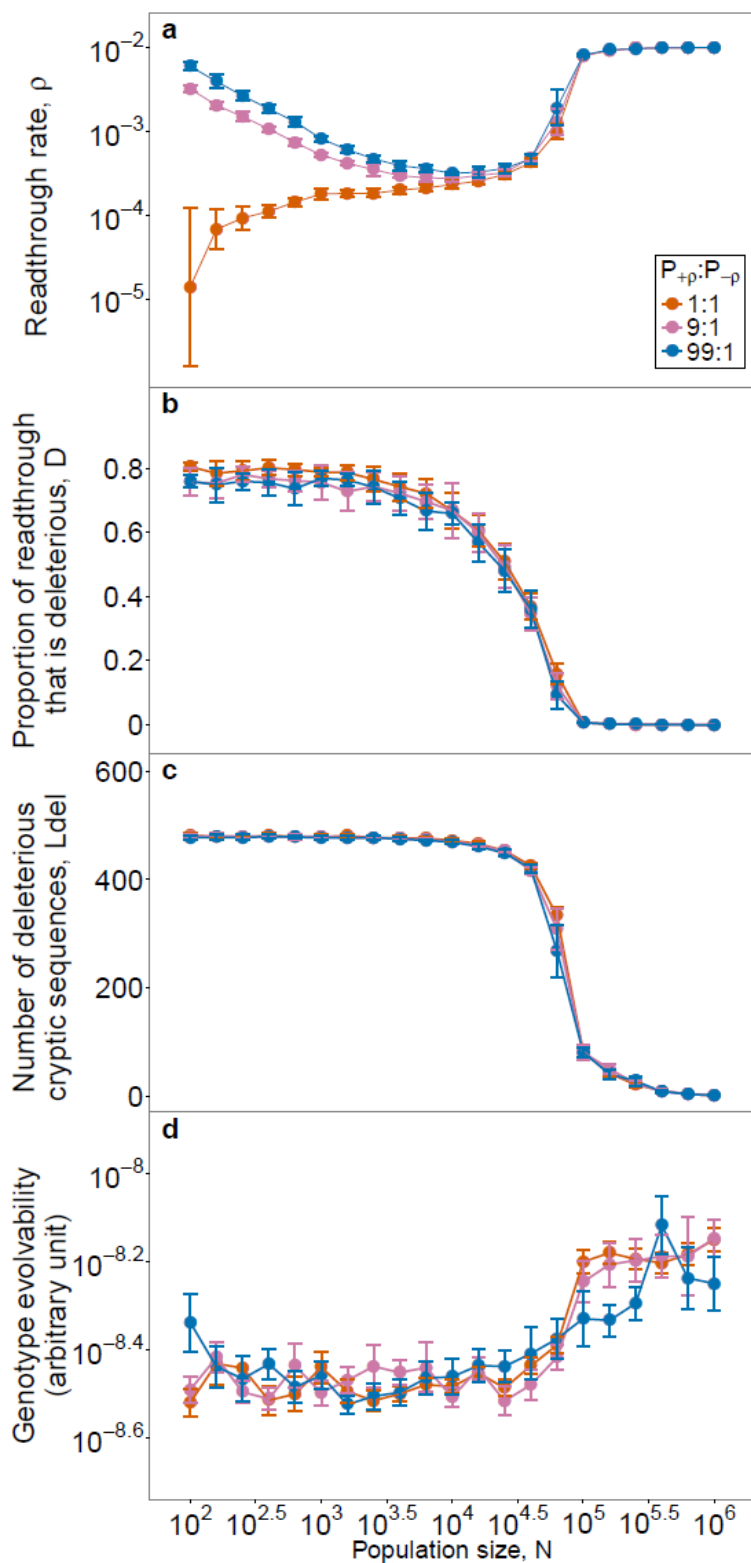


**Figure 4:** Mutation bias tends to increase  $\rho$ , such that even the global solution breaks down in sufficiently small populations.  $P_{+\rho}$  is the probability that a mutation increases  $\rho$ , and  $P_{-\rho}$  is the probability of a decrease. Each data point, (except those taken from Fig. 1 with  $P_{+\rho}:P_{-\rho} = 1:1$  and  $N = 10^{3.6}$  to  $N = 10^{6.0}$ ), is pooled from 5 replicates of high- $\rho$  initial conditions and 5 replicates of low- $\rho$  initial conditions. Because we assume multiplicative mutational effects to  $\rho$ , its value converges even for extremely small  $N$ . I.e., as  $\rho$  increases, the additive effect size  $\Delta\rho$  of a typical mutation also increases, preventing it from passing through the drift barrier. For **a**, **b**, and **c**, data is shown as mean  $\pm$  SD. For **d**, data is shown as mean  $\pm$  SE. For **a** and **d**, these apply to log-transformed values.  $L = 600$  and  $\sigma_E = 2.25$ .

## **Supplemental material for the manuscript**

### **“Drift barriers to quality control when genes are expressed at different levels”**

Xiong K, McEntee JP, Porfirio DJ, Masek J

## Implementation of origin-fixation simulations

Origin-fixation models are often implemented via a crude rejection algorithm; large numbers of mutations are simulated, and each is accepted as a successful fixation event if and only if a random number sample from the uniform [0, 1] distribution falls below its (fairly low) fixation probability. For large  $N$ , this method is computationally slow when significant numbers of nearly neutral mutations must be sampled before one fixes with probability  $\sim 1/N$ . Given that our model posits only a relatively small range of possible mutations, we instead sampled only mutations that go on to become fixed, by sampling according to the relative values of “fixation flux”, proportional to mutation rate  $\times$  fixation probability for each of our six categories of mutation. In other words, we used a form of the Gillespie (1977) algorithm.

In a haploid population of size  $N$ , the probability of fixation of a new mutant into a resident population is given by

$$P_{fix} = \frac{1-e^{-s}}{1-e^{-Ns}} \quad (9)$$

where  $s = w_{mutant}/w_{resident}-1$ . It is then straightforward to calculate fixation flux values for all possible switches between benign and deleterious states:

$$f_{del\_to\_ben} = N\mu_{ben} \sum_{i \in loci\_with\_del\_crypt\_seq} P_{fix}(del\_to\_ben\_at\_i) \quad (10)$$

$$f_{ben\_to\_del} = N\mu_{del} \sum_{i \in loci\_with\_ben\_crypt\_seq} P_{fix}(ben\_to\_del\_at\_i) \quad (11)$$



Matters are slightly more complicated for quantitative mutations to  $\alpha$ ,  $\beta$  and  $\rho$ , because we must integrate the fixation flux over all possible sizes ( $\Delta\alpha_k$ ,  $\Delta\beta_k$ , and  $\Delta\log_{10}\rho$ ) for a mutation at a given locus, prior to summing across loci to arrive at the fixation flux for an entire mutational category:

$$f_\alpha = N\mu_\alpha \sum_k^K \int P_{fix}(\Delta\alpha_k)P(\Delta\alpha_k)d\Delta\alpha_k \quad (12)$$

$$f_\beta = N\mu_\beta \sum_k^K \int P_{fix}(\Delta\beta_k)P(\Delta\beta_k)d\Delta\beta_k \quad (13)$$

$$f_\rho = N\mu_\rho \int P_{fix}(\Delta\log_{10}\rho)P(\Delta\log_{10}\rho)d\Delta\log_{10}\rho \quad (14)$$

where  $P(\Delta\alpha_k)$ ,  $P(\Delta\beta_k)$ , and  $P(\Delta\log_{10}\rho)$  are the probability densities for the magnitude of a given kind of mutation.

We use the quadrature method to calculate the integral over these possibilities, using a grid of 2000, limited for  $\Delta\alpha_k$  to the interval  $[-\alpha_k/a-5\sigma_m/K, -\alpha_k/a+5\sigma_m/K]$ , for  $\Delta\beta_k$  to the interval  $[-\beta_k/a-5\sigma_m/K, -\beta_k/a+5\sigma_m/K]$ , and for  $\Delta\log_{10}\rho$ , to the interval  $[-10\sigma_\rho, \min(10\sigma_\rho, -\log_{10}\rho)]$ . In the latter case, the number of grid intervals is reduced proportional to any truncation of the interval at  $-\log_{10}\rho$ .

For mutational co-options of benign cryptic sequences, the effect of replacing the value of  $\alpha_k$  with that of  $\alpha_k + \beta_k$  is fixed, but there is also a stochastic range of effects of initializing a new  $\beta_k$  and a new  $B_k$  (Eq. 15). Let  $P(\beta'_k)$  be the probability density of a new  $\beta_k$  given by Normal(0,  $V(a, K, \sigma_m)$ ), and  $P(B'_k = 1) = 1 - P(B'_k = 0)$  be the probability that a new  $B_k$  equals to 1, and hence the new  $\beta_k$  affects the trait value. The fixation flux associated with cooption mutations we obtained numerically by integration over the range  $[-5\sigma_m/K, 5\sigma_m/K]$ :

$$f_{coopt} = N\mu_{coopt} \sum_{k \in \text{loci\_with\_ben\_crypt\_seq}}^K \left( P(B'_k = 1) \int P_{fix}(\beta'_k, B'_k = 1) P(\beta'_k) d\beta'_k + P(B'_k = 0) P_{fix}(B'_k = 0) \right) \quad (15)$$

The expected waiting time before the current genotype is replaced by another is

$$\text{waiting time} = \frac{1}{\text{total fixation flux over all six categories}} \quad (16)$$

A standard Gillespie (1977) algorithm would calculate the realized waiting time as a random number drawn from an exponential distribution with this mean. Since we are only interested in the outcome of evolution, and not the variation in its timecourse, we used the expected waiting time instead, decreasing our computation time. The waiting time can be interpreted as the time it takes for a mutation destined for fixation to appear, neglecting the time taken during the process of fixation itself. Using this interpretation, we specify waiting times in terms of numbers of generations, based on our assumptions about absolute mutation rates.

We assign the identity of the next fixation event among the six categories according to probabilities proportional to their relative fixation fluxes, then we assign the identity within the category. For switches between benign and deleterious states, allocating a fixation event within a category according to the relative values of fixation fluxes is straightforward. For mutations to  $\rho$ ,  $\alpha$ , and  $\beta$ , and mutational co-option, we relax the granularity and cutoff assumptions of the grid-integration method when choosing a mutation within the category. Instead, we sample a mutational value of  $\Delta\log_{10}\rho$  from  $\text{Normal}(\rho_{bias}, \sigma_{\rho}^2)$ . We reject and resample  $\Delta\log_{10}\rho$  if  $\Delta\log_{10}\rho \geq -\log_{10}\rho$ . Otherwise, we accept vs. reject-resample according to the fixation probability of that exact mutation, by comparing this probability to a random number uniformly distributed at  $[0, 1.1 \times \text{the maximum fixation probability across the grid points previously calculated for } \Delta\log_{10}\rho \text{ during our grid calculation}]$ . For  $\Delta\alpha$  (or  $\Delta\beta$ ), the procedure is conceptually similar but has a more complicated implementation. We first sample from  $\text{Normal}(0, (\sigma_m / K)^2)$ . We then add the random number to each of the values of  $-\alpha_k/a$ , and calculate the sum of corresponding fixation probabilities across all loci  $k$ . We accept vs. reject-resample the mutation by comparing this sum to a random sample from a uniform distribution at  $[0, 1.1 \times \text{the maximum corresponding fixation probability sum calculated during our grid calculation}]$ . If the mutation is accepted, we allocate it to a locus  $k$  with probability proportional to their relative fixation probabilities. For mutational co-option of a benign cryptic sequence, the main effect is to replace  $\alpha_k$  with  $\alpha_k + \beta_k$ , but there are also subtler effects arising from the reinitialization of the new cryptic sequence. Any of the  $k$  loci for which  $B = 1$  are eligible for co-option, the new value of  $B$  may be either 0 to 1, and the new  $\beta_k$  may take a range of values. Each combination of  $k$  and new  $B$  has its own fitness flux, and the first choice is among these  $\{k, B\}$  pairs. Next we sample

$\beta_k$  from Normal(0,  $(\sigma_m/k)^2$ ); for a new  $B$  equal to 0 we always accept the result, and for new  $B$  equal to 1, we accept vs. reject-resample  $\beta_k$  by comparing its probability of fixation to a random sample from a uniform distribution at  $[0, 1.1 \times \text{the maximum corresponding fixation probability sum calculated during our grid calculation}]$ .

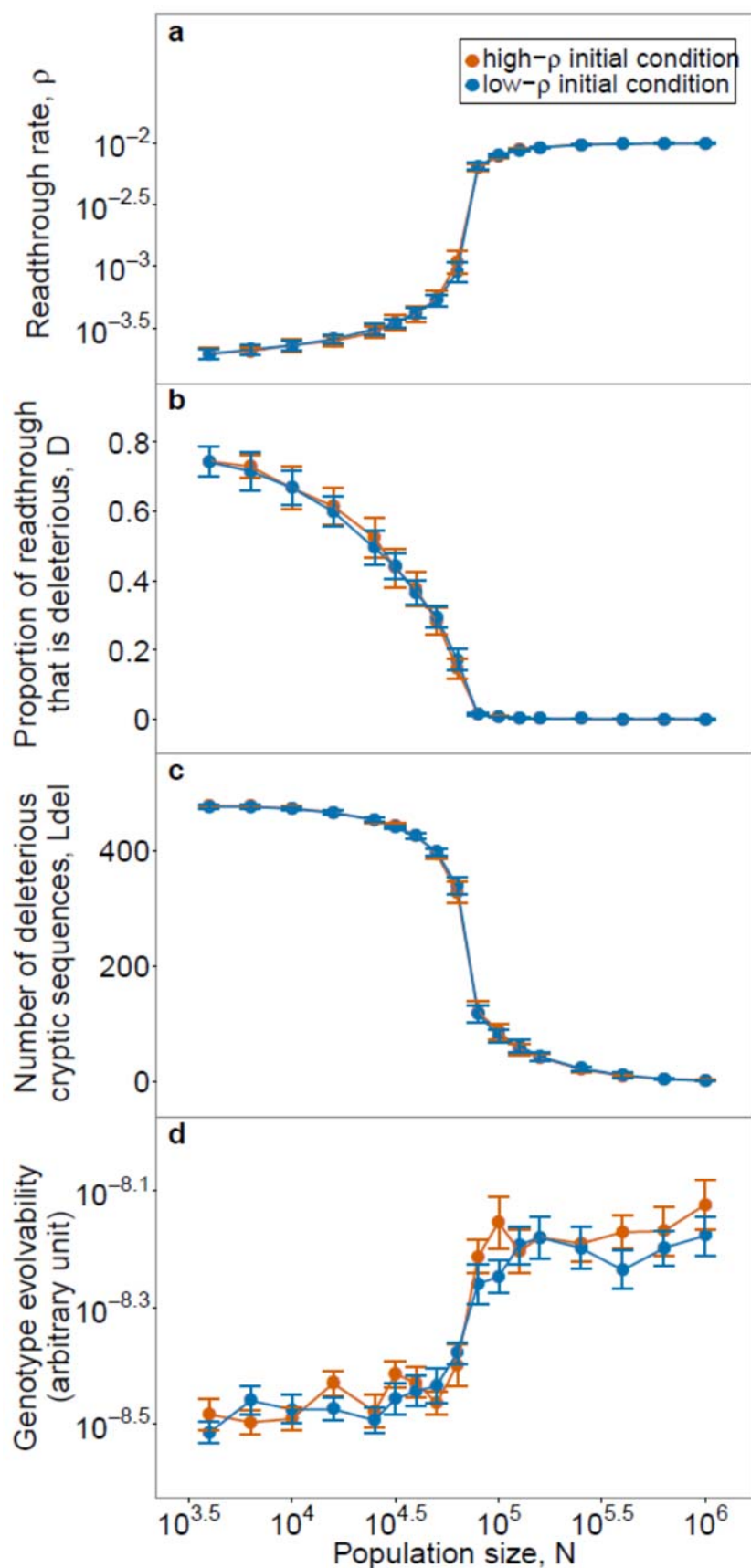


**Figure S1:** At  $\sigma_E = 2.25$ , the final state of the evolutionary simulation does not depend on the initial conditions. The data shown here is the same as that shown pooled in Fig. 1.

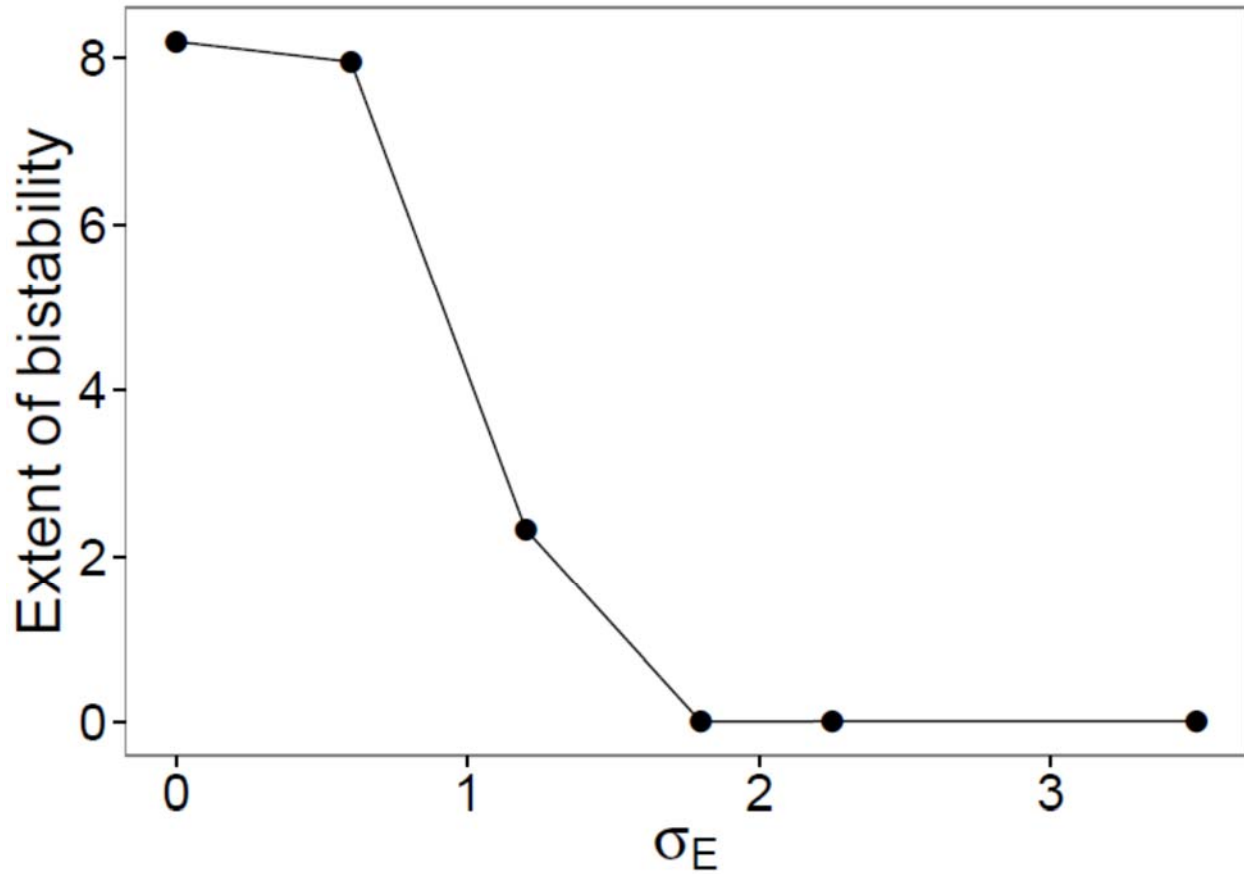


**Figure S2:** The range of population sizes that exhibit significant bistability drops dramatically even for  $\sigma_E < 2.25$ . We used average values of  $\rho$  towards the end of the simulations as a measure of the solution found by each replicate. For each initial condition, we averaged over five replicates (except for  $\sigma_E = 0, 2.25$ , and  $3.5$ , where we reused the 20 replicates of Fig. 1), and over each of the values of  $N$  between  $10^{3.6}$  to  $10^6$ , with an increment of  $10^{0.2}$ . The extent of bistability was assessed as  $\sum_N (\log_{10} \bar{\rho}_{init\_low} - \log_{10} \bar{\rho}_{init\_high})^2$ .  $L = 600$ .

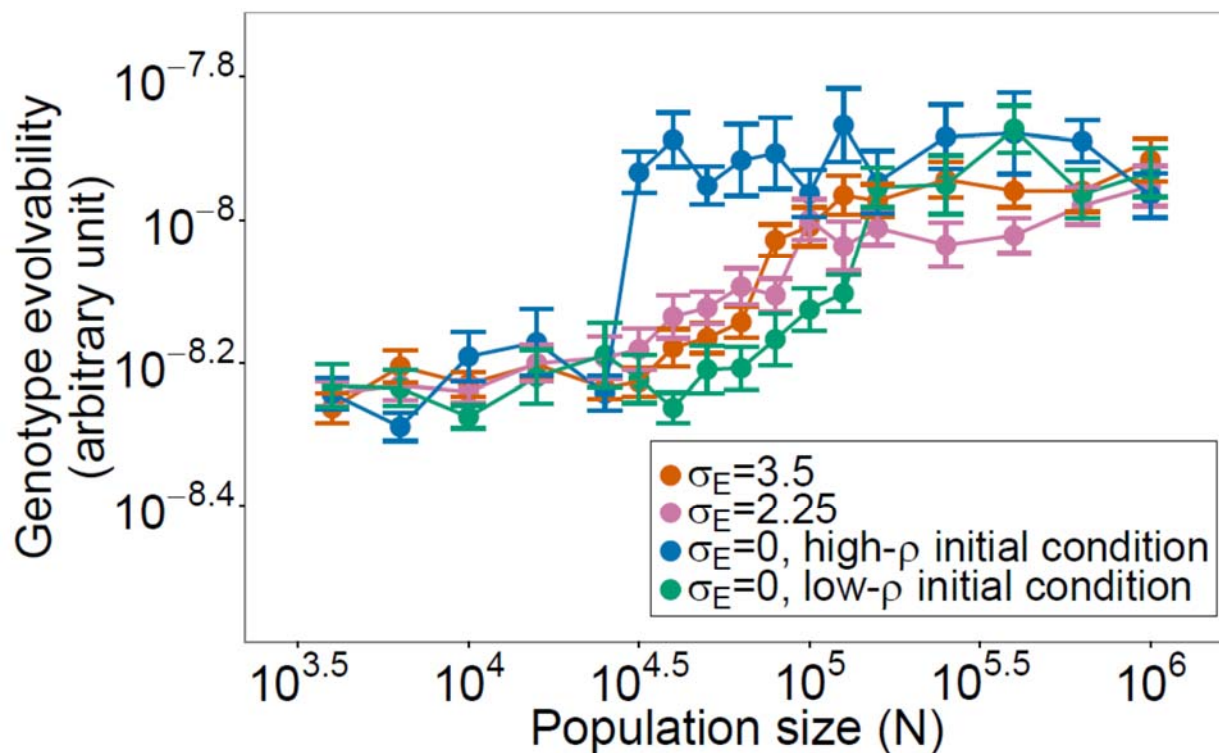


**Figure S3:** The time taken for the trait to approach the new value of  $x_{opt}$  behaves similarly to the recovery time of fitness shown in Fig. 1d. The same simulations were used as in Fig. 1. At  $\sigma_E = 2.25$  and  $\sigma_E = 3.5$ , we pooled the results from high- $\rho$  and low- $\rho$  conditions. Evolvability is shown as mean  $\pm$  SE of the log-transformed values.  $L = 600$ .

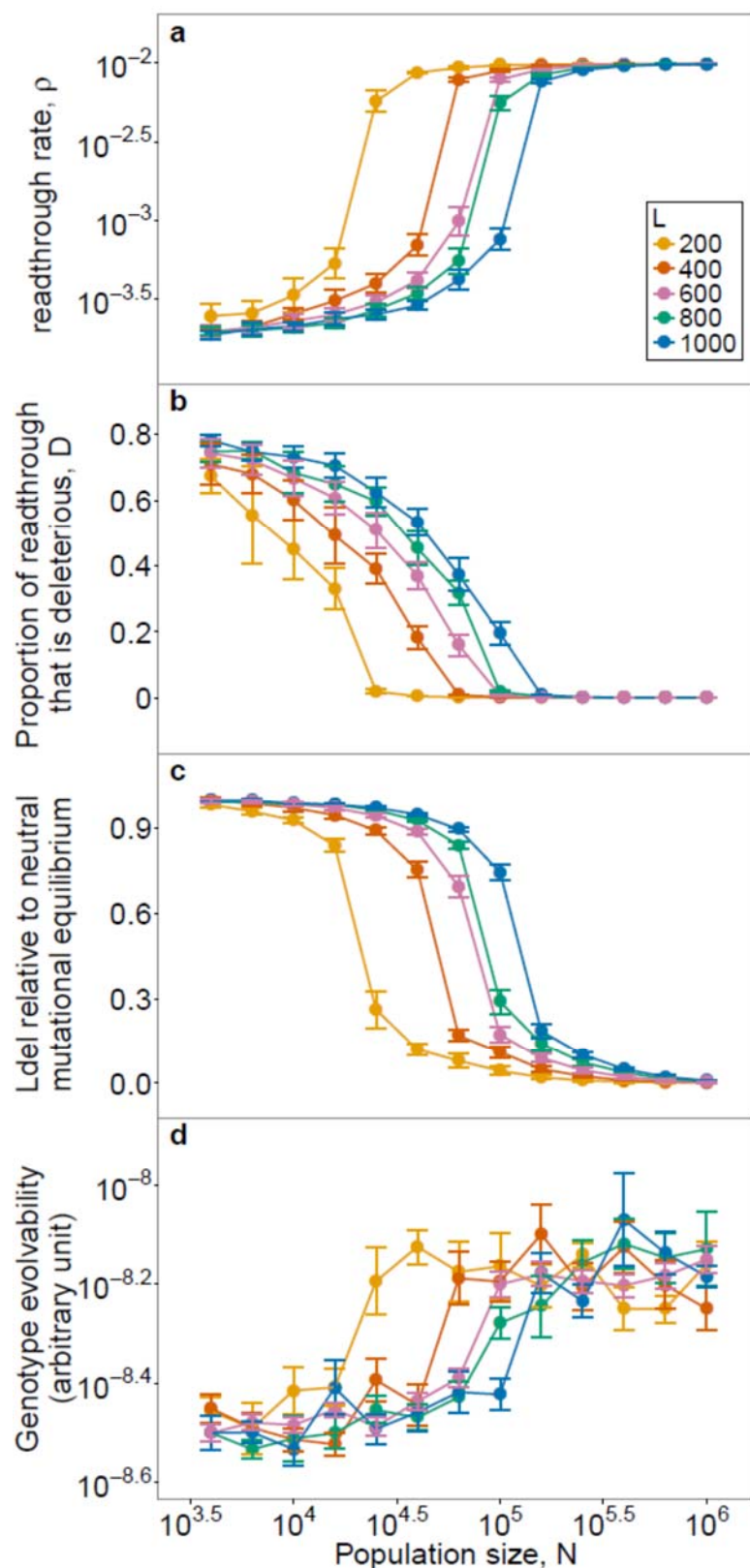


**Figure S4:** Changing the number of loci does

not qualitatively change our results.

Quantitatively, fewer loci favor more local

solutions. Changing  $L$  alters the average

contribution of each locus to  $D$ . This alters the

average strength of selection on each locus,

independent of population size. Therefore, the

same solutions, characterized by the values of

$\rho$  and  $D$ , are “shifted” to small values of  $N$  as  $L$

decreases. While  $L$  changed, we held the

number of quantitative trait loci constant at

50. For  $L = 600$ , we reused the results shown

in Fig. 1. For other values of  $L$ , five replicates

were run for each of the two initial conditions.

We pooled results from both initial conditions

across all values of  $L$ . We normalized  $L_{del}$  to the

neutral mutational equilibrium of

$L \times \mu_{del} / (\mu_{del} + \mu_{ben})$ . For panels **a** to **c**, data is

shown as mean  $\pm$  SD. For **d**, data is shown as

mean  $\pm$  SE. For **a** and **d**, these apply to log-

transformed values.  $\sigma_E = 2.25$ .



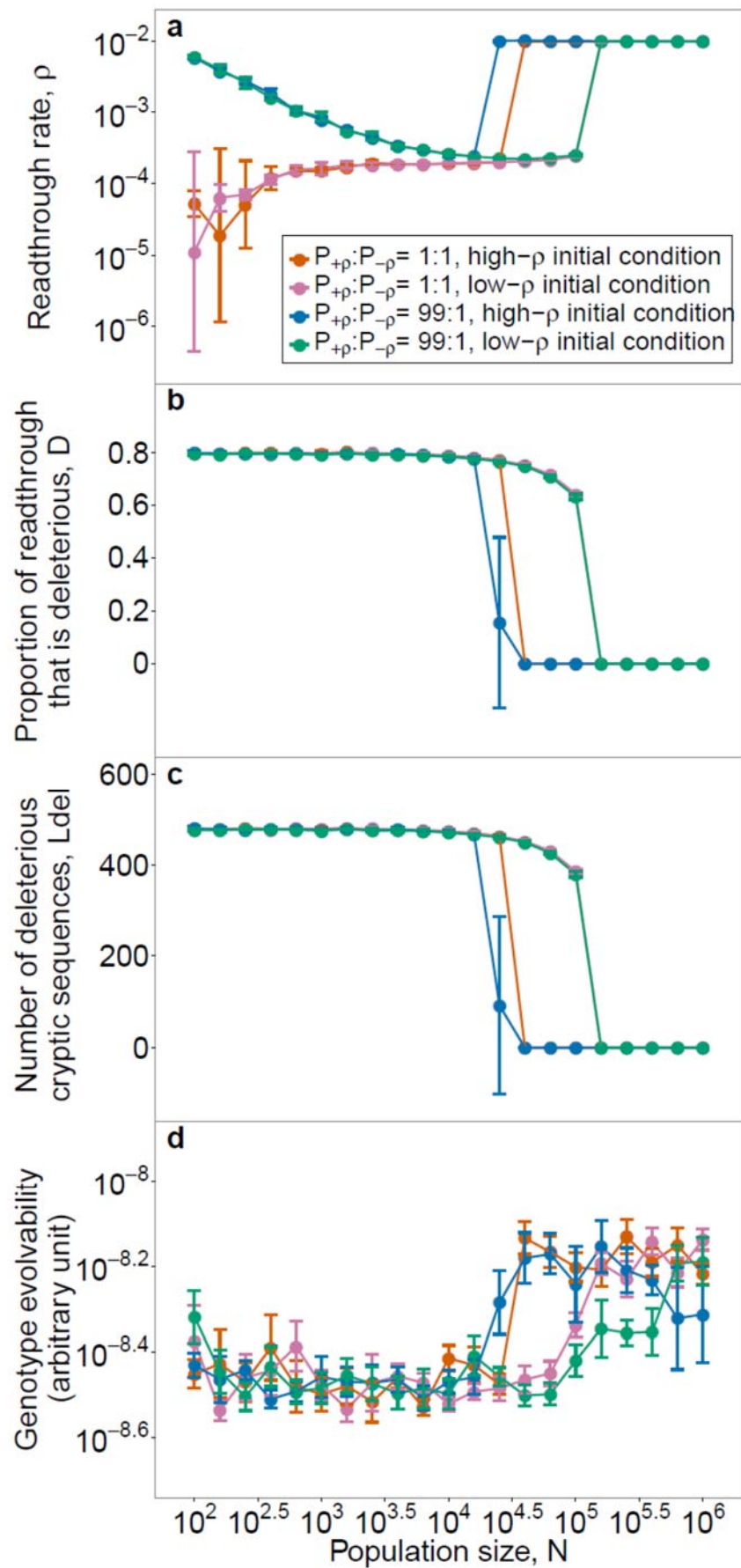


**Figure S5:** Fig. 4 results (that the global solution breaks down in sufficiently small populations) remain true in the absence of variation of expression levels. Data points between  $N = 10^{3.6}$  to  $N = 10^{6.0}$  and  $P_{+\rho}:P_{-\rho} = 1:1$ , are reused from Fig. 1; for the others, we performed 5 replicates for each condition. For panels **a** to **c**, data is shown as  $\text{mean} \pm \text{SD}$ . For **d**, data is shown as  $\text{mean} \pm \text{SE}$ . For **a** and **d**, these apply to log-transformed values.  $L = 600$ .

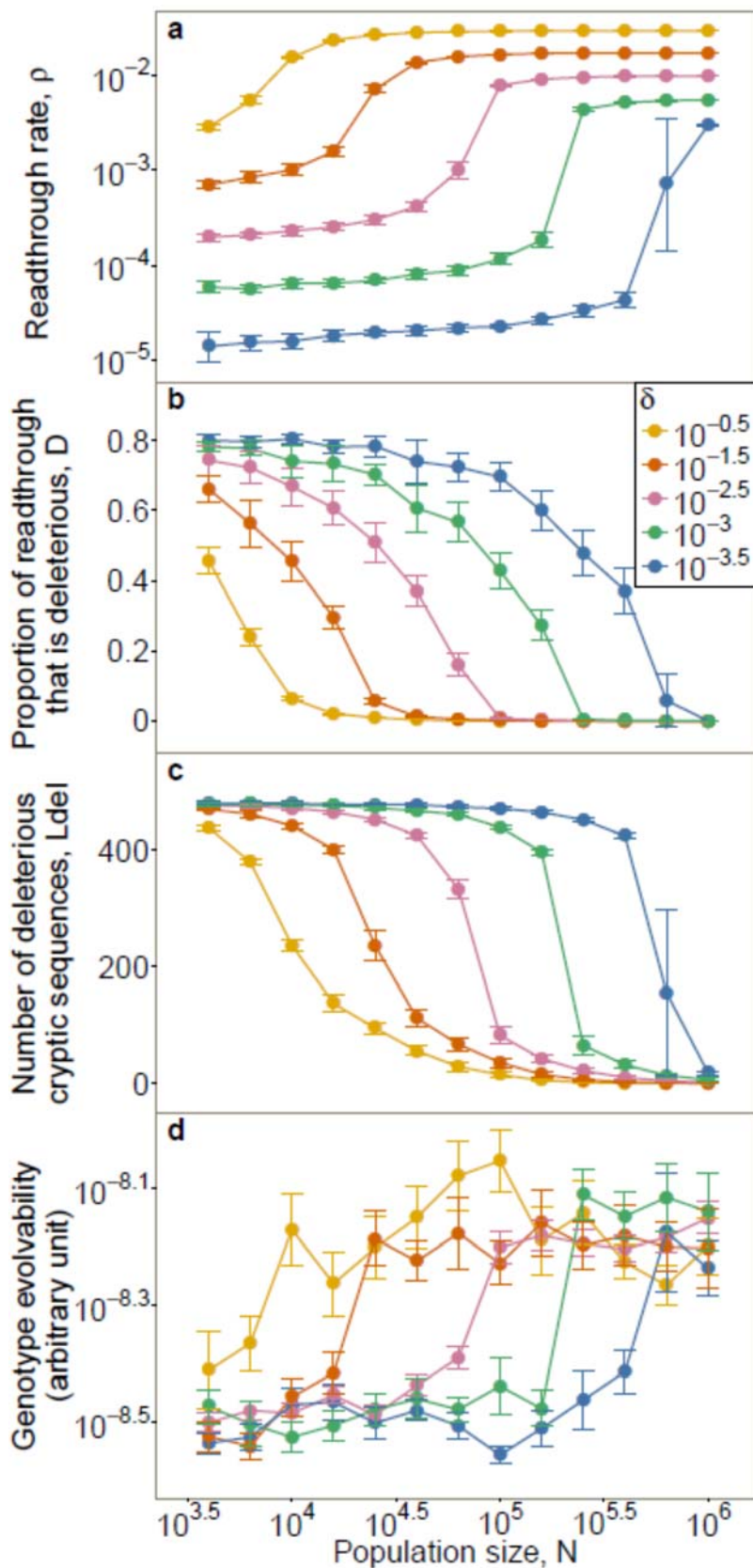


**Figure S6:** Increasing the cost of quality control  $\delta$  expands global solutions to smaller populations and reduces the differences in error rates as a function of population size. For  $\delta = 10^{-2.5}$ , we reused the data from Fig. 1; for each of the other values of  $\delta$ , we ran 5 replicates from the high- $\rho$  initial condition and 5 from the low- $\rho$  initial condition. Each data point represents the pooled results from the two initial conditions. For panels a to c, data is shown as mean  $\pm$  SD. For d, data is based on time to fitness recovery and is shown as mean  $\pm$  SE. For a and d, the mean, SD and SE are calculated on log-transformed values. The large error bars at  $N = 10^{5.8}$  under  $\delta = 10^{-3.5}$  across all panels are due to different initial conditions, which is a sign of bistability.  $L = 600$ ,  $\sigma_E = 2.25$ .

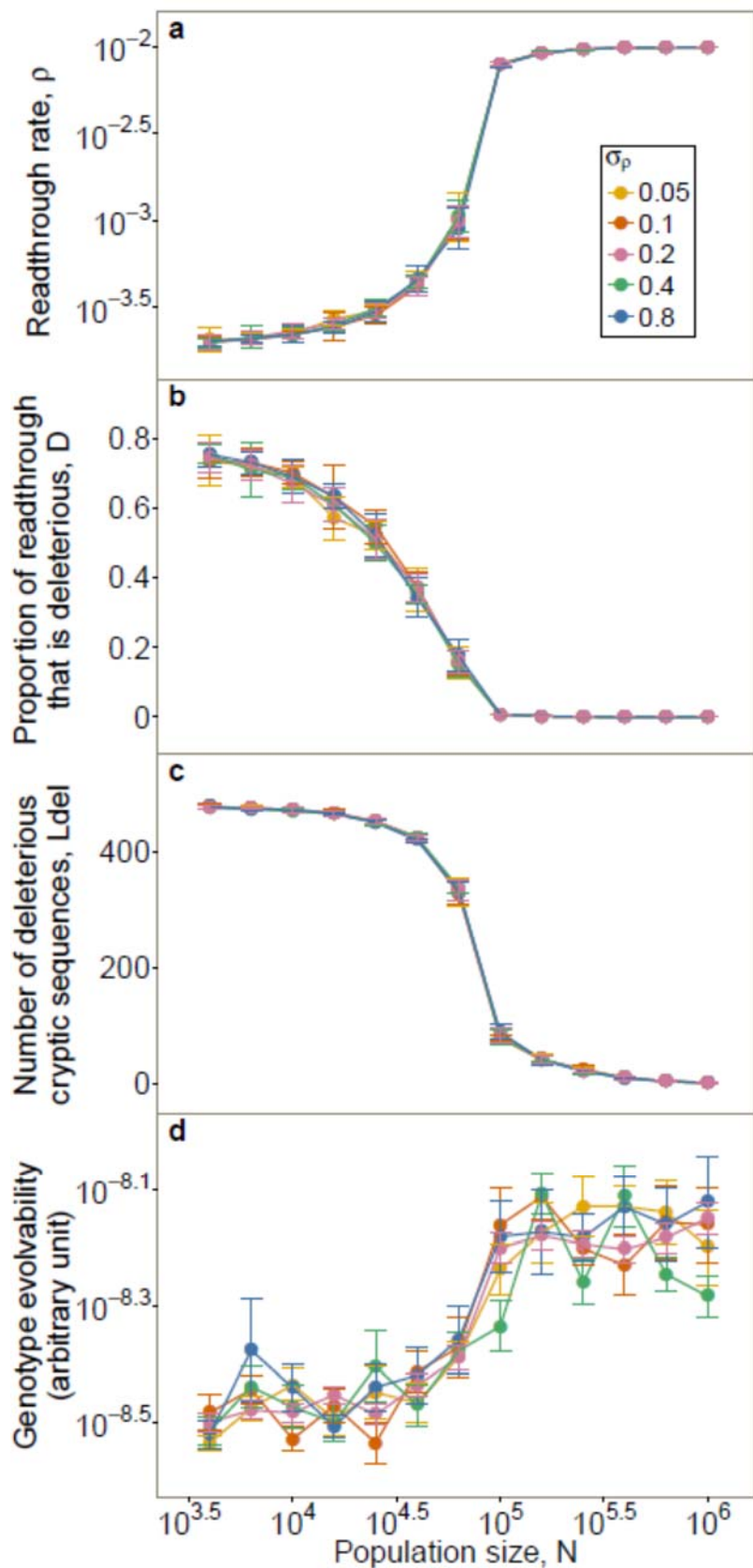


**Figure S7:** The variance in the magnitude of mutations to  $\rho$  does not affect a population's solution to error or evolvability. For  $\sigma_\rho = 0.2$ , we reused the data from Fig. 1; for each of the other values of  $\sigma_\rho$ , we ran 5 replicates from each of the two initial conditions. We pooled results from the two initial conditions for each data point. For panels a to c, data is shown as mean  $\pm$  SD. For d, data is based on time to fitness recovery and is shown as mean  $\pm$  SE. For a and d, these apply to log-transformed values.  $L = 600$ ,  $\sigma_E = 2.25$ .

**Table S1: Summary of model parameters**

Group	Parameter	Biological meaning	Exploration	Parameter values in model <sup>[1]</sup>	Influence on global v. local solutions
Selection for local vs. global solution	$\sigma_E^2$	Variance of $\log_2$ expression among loci	Fig. 1, Fig. S2	5.1 (0-12.3)	Central finding: lower $\sigma_E^2$ promotes dichotomy
	$c$	Cost of misfolding	Fig. S3 <sup>[2]</sup>	20 (7-28 <sup>[2]</sup> )	Large $c$ makes $\rho$ smaller, with a slightly larger impact on global solutions, and expands the bistable region to smaller populations.
	$\delta$	Scaling of quality control costs	Fig. S6	$10^{-2.5}$ ( $10^{-0.5}$ - $10^{-3.5}$ )	Higher cost makes $\rho$ larger, with a larger impact on global solutions, and expands global solutions to smaller populations
	$L$	Total number of loci	Fig. S4, Fig. S2 <sup>[2]</sup>	600 (200-1000)	Lower $L$ shift the transition between local and global solutions to smaller populations, but maintain the shape of the transition
Mutation bias for local vs. global solution	$\mu_{del}$	Rate of benign-to-deleterious mutations	Fig. 3	$\mu_{del}:\mu_{ben} = 4:1$ (1:1-99:1)	Stronger mutation bias lowers $\rho$ and shifts the transition between local and global solutions to larger populations
	$\mu_{ben}$	Rate of deleterious-to-benign mutations			
	$P_{+\rho} \times \mu_\rho$	Rate of mutations that increase $\rho$	Fig. 4, Fig. S5	$P_{+\rho}:P_{-\rho} = 1:1$ (1:1-99:1)	Mutation bias prevents extremely small populations from reducing $\rho$
	$P_{-\rho} \times \mu_\rho$	Rate of mutations that decrease $\rho$			
Relevant only for quantitative effects and evolvability (of peripheral interest to our central findings)	$\sigma_\rho^2$	var(mutations to $\rho$ )	Fig. S7	0.04 ( $2.5 \times 10^{-3}$ -0.64)	No apparent influence
	$K$	Number of quantitative trait loci	Fig. S7 <sup>[2]</sup>	50 (5-50 <sup>[2]</sup> )	
	$a$	Speed that $\alpha$ and $\beta$ revert to mean	Fig. S10 <sup>[2]</sup>	750 (250-2000 <sup>[2]</sup> )	
	$\mu_{coopt}$	Rate of co-option mutations	-	$2.56 \times 10^{-9}$	
	$\mu_\alpha$	Rate of mutations to $\alpha$	-	$3 \times 10^{-7}$	
	$\mu_\beta$	Rate of mutations to $\beta$	-	$3 \times 10^{-8}$	
	$\sigma_m^2$	$\sigma_m^2/K = \text{var}(\text{mutations to } \alpha \text{ and } \beta)$	Fig. S8 <sup>[2]</sup>	0.25 (0.04-1 <sup>[2]</sup> )	
$\sigma_f$	Strength of selection on trait	No loss of generality when $\sigma_m^2$ only is explored		0.2	

<sup>[1]</sup>The numbers outside parentheses are the default values and the numbers inside indicate the parameter range explored.

<sup>[2]</sup>Rajon and Masel (2011)

## Supplementary References:

Rajon, E., and J. Masel, 2011 The evolution of molecular error rates and the consequences for evolvability. *Proc. Natl. Acad. Sci. U.S.A.* 108: 1082-1087.